On cochlear encoding: Potentialities and limitations of the reverse-correlation technique

E. de Boer, and H. R. de Jongh

Citation: The Journal of the Acoustical Society of America **63**, 115 (1978); doi: 10.1121/1.381704
View online: http://dx.doi.org/10.1121/1.381704
View Table of Contents: http://asa.scitation.org/toc/jas/63/1
Published by the Acoustical Society of America

On cochlear encoding: Potentialities and limitations of the reverse-correlation technique

E. de Boer and H. R. de Jongh

Physics Laboratory ENT Department (KNO) Wilhelmina Hospital Amsterdam, The Netherlands
(Received 29 November 1976; revised 27 June 1977)

This paper presents a description of the interrelation between two major properties of the responses recordable from auditory nerve fibers: *frequency selectivity* and *partial synchrony* between stimulus and response. In the course of this work the influence of nonlinearity on the cochlear encoding process can be assessed. The theory of the *reverse-correlation technique* is derived in a most general way. It is based on a model in which a filter—assumed to be linear—is followed by a stochastic pulse generator—the probability of producing an output pulse being an instantaneous but nonlinear function of its input signal. Insofar as such a model represents stimulus transformations in a primary auditory neuron, the technique can be applied to the responses recorded from an auditory nerve fiber. Several illustrative examples of experimental reverse-correlation functions—abbreviated: *revcor functions*—are presented and discussed. These functions have the general character of impulse responses of sharp bandpass filters. They show very little phase modulation. For noise stimuli of up to 70 dB per third octave the revcor functions are almost invariant. Above that level some (but not all) of the revcor functions show a loss of frequency selectivity. If a nerve fiber can be contacted for a sufficiently long time, it is possible to compare the response with that of a model filter, in which the revcor function of that fiber is substituted as its impulse response. The output signal of the model filter is shown to be a very good predictor of the firing probability of the fiber under study. This property is demonstrated for noise as well as for tone stimuli. There is surprisingly little evidence of nonlinear filtering in these results. This so-called simulation method can also be applied when the stimulus is switched on and off. The results show, apart from effects due to filtering, clear manifestations of fast adaptation. Again, the filtering appears to be independent of the latter effect. It is concluded that for wide-band noise and single-tone signals the firing probability is predominantly controlled by a linearly filtered version of the acoustical stimulus; this constitutes the principle of *specific coding*. The conspicuous absence of nonlinear effects in the results can partly be explained in terms of the response properties of a class of networks in which sharp filtering occurs after the generation of nonlinear distortion products. It can then be predicted that this property will hold only for wide-band and tonal stimuli. That our results show so little evidence of cochlear distortion appears to be a property of signal transformations and is not due to linearization tendencies of the experimental method.

PACS numbers: 43.63.Pd, 43.63.Bq, 43.63.Nc, 43.63.Rf

INTRODUCTION

In the past decades many studies have been dedicated to the response properties of single auditory-nerve fibers (primary auditory neurons[1]). In this paper we will describe the relation between two of the main properties, namely frequency selectivity and time locking (synchrony), as revealed by the application of modern on-line computing techniques. The results described in the paper extend the concept of partial synchrony between stimulus and response to include stimulation with stochastic and with nonstationary signals: noise and tone bursts. It is shown that for each neuron a linear transform of the stimulus can be constructed in such a way that the nerve fiber's firings show a great deal of synchrony with it. For the type of stimuli used, this confirms the validity of a model of a primary auditory neuron which contains a linear filter as the only frequency-selective part. The model can be used as a functional model: i.e., it can predict input–output relations in detail (input being the acoustical input to the ear and output the train of action potentials in a nerve fiber). A large number of such models, each representing a group of primary auditory neurons, can serve as a simplified representation of the cochlear encoding process.

The frequency selectivity that responses of auditory-nerve fibers exhibit is usually described in terms of tuning curves, determined for pure-tone stimuli. (See e.g., Kiang *et al.*, 1965; Evans, 1972.) A tuning curve shows the boundary along which a certain increase in spike rate due to the presence of the stimuli is observed. As a result of several nonlinear phenomena the curves determined for different increases in spike rate above the spontaneous rate are not parallel (e.g., Rose *et al.*, 1967).

A second important property of auditory-nerve fibers is the partial synchrony of the firings with the waveform of the stimulus (Hind *et al.*, 1967; Anderson *et al.*, 1971; de Jongh, 1972). There is a limit to the synchrony between stimulus and response: For stimuli above 6 kHz the effect can no longer be demonstrated. This limiting behavior does not seem to be due to errors or inaccuracies in the measurement of the epochs of nerve-fiber action potentials, but to an intrinsic timing limitation in the nervous excitation process.

The third property of cochlear transduction which is reflected by the response pattern of auditory-nerve fibers is nonlinearity (Sachs and Kiang, 1968; Sachs, 1969; Goldstein and Kiang, 1968; Goblick and Pfeiffer, 1969). See for a review paper Pfeiffer and Kim, 1973.

To these nonlinear phenomena we may add properties

 0001-4966/78/6301-0115$00.80

that seem to be mainly of a typical neural character, such as adaptation (e.g., Smith, 1973), saturation (Kiang *et al.*, 1965), and the depletion effect described by Gray (1966). This is certainly a bewildering situation, and we may well ask what type of simple model will describe the encoding for everyday signals such as animal cries and human speech.

In this paper it will be shown to what extent the properties frequency selectivity and synchrony can be tied together by a *linear* type of model. For linear systems it is possible to extract the parameters by operations on stochastic input and output signals. Such a technique can also be used to extract the dynamic response characteristics from a stochastic, frequency-selective system that accepts an analog signal as input signal and produces a series of impulses at the output—the technique of triggered correlation (de Boer and Kuyper, 1968). The application of this technique to cochlear physiology is known as reverse correlation (de Boer, 1967, 1968, 1969a, 1969b; de Boer and Jongkees, 1968). The method involves stimulation of the ear of an experimental animal (cat) with white noise, recording of the train of action potentials from a single fiber of the auditory nerve, and computation of a specific type of cross-correlation function. For each fiber the result comes in the form of a time function, which can be associated with the nerve fiber studied. That function is known as the "revcor function" (reverse-correlation function) of the fiber. The Fourier transform of a revcor function has the character of a bandpass-filter frequency response; the corresponding frequency response function has extremely steep slopes and, in fact, is very similar to the pure-tone tuning curve (de Boer, 1973). Section I of the present paper presents the derivation of the theory in a most general way and reports the waveshapes of typical revcor functions for a number of primary auditory neurons.

In view of the many and strong nonlinearities in the cochlea it seems at first sight not fruitful to pursue a linear analysis too far. It is shown in Secs. II and III, however, how well the revcor function of a nerve fiber can be used to predict detailed temporal properties of the fiber's response to wide-band signals and tonebursts. For this purpose the response of the actual physiological preparation is compared with that of a model in which a linear filter is the only frequency-selective element. The revcor function is substituted as the impulse response of this filter. It is found that the firing probability of the neuron is nearly proportional to the rectified output of the filter, this holds true for neurons with resonance frequencies (CF's) of 2 kHz and lower. For neurons with higher resonance frequencies the firing probability behaves as a linear (low-pass) transform of the rectified output of the model filter. The success of this so-called "simulation procedure" can be interpreted to mean that the neural transducer mainly reacts to a linearly filtered version of the stimulus, the so-called principle of specific coding (de Boer, 1973), and that in the cochlear filtering process, nonlinear effects are not very important. This conclusion is subject to the restriction of wide-band stimulus signals and single pure tones and it cannot be expected to hold true for signals with steep slopes in their spectrum (single-sideband signals and tone complexes).

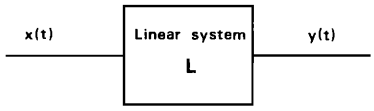

FIG. 1. Linear system driven by a stochastic signal.

For stimuli with an abrupt onset the picture is complicated by adaptation. The influence of this effect can easily be separated from the filtering process and again there appears very little evidence of nonlinear filtering. In other words, nonlinear filtering or time-varying effects do not substantially upset detailed temporal relations between the stimulus signal and the nerve fiber's firing probability. This holds true for stationary as well as transient wide-band stimulus signals and for tonebursts.

In Sec. IV several specific topics are discussed regarding the use of the revcor function and the consequences of the results. It is concluded that, as far as the prediction of firing patterns is concerned, the model with a linear filter is sufficient for describing cochlear encoding for most if not all signals occurring in everyday life. A tentative explanation is offered for the observed near-invariance of revcor functions for variations in stimulus intensity. Furthermore, the conspicuous absence of nonlinear filtering effects is discussed in terms of the BPNL network (de Boer, 1976a). As far as cochlear filtering is concerned, nonlinear effects appear to be of a type that leaves hardly a discernible trace in the processing of wide-band signals. This is consistent with the idea that nonlinear effects occur on a "wide-band" basis and that the distortion products generated are affected by sharp bandpass filtering. However, this is not the only possible explanation.

I. REVCOR FUNCTIONS; THEORY AND EXPERIMENTS

We first derive the basic theory behind the reverse correlation technique. Note that the present derivation differs from the one used when the method was originally derived (de Boer and Kuyper, 1968). Consider a linear system L (Fig. 1) with a stochastic signal $x(t)$ at its input terminals, and let $y(t)$ be the output signal. The cross-correlation function $\varphi_{xy}(\tau)$ is defined as the time (or ensemble) average of the product $x(t+\tau)\times y(t)$:

$$\varphi_{xy}(\tau) = \overline{x(t+\tau)\times y(t)} \,, \tag{1}$$

where the bar indicates the averaging operation. For the system of Fig. 1 the following relation holds:

$$\varphi_{xy}(\tau) = \int_0^\infty \varphi_{xx}(\tau+\sigma)\times h(\sigma)\, d\sigma \,, \tag{2a}$$

where $\varphi_{xx}(\tau)$ is the auto-correlation function of $x(t)$ and $h(t)$ is the impulse response of the linear system L. If white noise is chosen for $x(t)$, the relation becomes particularly simple

$$\varphi_{xy}(\tau) = h(-\tau) \,. \tag{2b}$$

The system of Fig. 2 is more complex; it can be used as a model for a primary auditory neuron[1] to describe the transformation of the acoustic stimulus signal $x(t)$ into a train $s(t)$ of impulses recordable from the pertinent nerve fiber (cf. Siebert, 1968; Duifhuis, 1972). The probability of firing $p(t)$ of the pulse generator PG is assumed to be a no-memory nonlinear transform of the signal $y(t)$ produced by L. For this system the cross-correlation function $\varphi_{xs}(\tau)$ can conveniently be defined as a time average

$$\varphi_{xs}(\tau) = \lim_{T\to\infty} \frac{1}{T} \int_0^T x(t+\tau)\, s(t)\, dt \,. \tag{3}$$

If $s(t)$ consists of a number of δ functions

$$s(t) = \sum_{i=1}^{\infty} \delta(t - t_i) \tag{4}$$

this can be reduced to

$$\varphi_{xs}(\tau) = \lim_{T\to\infty} \frac{1}{T} \sum_{i=1}^{N_T} x(t_i + \tau) \,, \tag{5}$$

where t_i $(i = 1, \ldots, N_T)$ denote the N_T instants at which nerve impulses are detected in the time interval T.

For the purpose of analysis, the system of Fig. 2 can be redrawn as in Fig. 3. Here the pulse generator is linear: The probability of firing $p(t)$ is proportional to its input signal $z(t)$. All nonlinearity is lumped into the no-memory nonlinear element NL which, in particular, ensures that the signal $z(t)$ never becomes negative. It is easy to understand that the cross-correlation function $\varphi_{xs}(\tau)$ is proportional to $\varphi_{xz}(\tau)$. According to Price's theorem (Price, 1958) the latter function is proportional to $\varphi_{xy}(\tau)$, at least when $x(t)$ is Gaussian—$y(t)$ is then Gaussian too. Hence

$$\varphi_{xs}(\tau) = C \times \varphi_{xy}(\tau) \,. \tag{6}$$

In terms of Eqs. (2) this means that for a composite system as depicted by Fig. 2, the waveshape of the linear system's impulse response $h(t)$ can be recovered from a correlation measurement on stochastic input and output signals. If $x(t)$ is a white-noise signal, the relation becomes

$$h(\tau) = C^{-1} \times \varphi_{xs}(-\tau) \,. \tag{7}$$

The function $\varphi_{xs}(-\tau)$, obtained with white-noise input, is the *reverse-correlation function*, abbreviated: *revcor function*.

Let us assume that the model of Fig. 2 represents a primary auditory neuron. Then the same analysis can be applied to measure the properties of the linear filtering stage. The appropriate experiment involves simultaneous observation of the analog input signal (preferably white noise) and the output signal, i.e., the series of action potentials ("events") recorded from a single auditory nerve fiber. The computation should be triggered by the fast initial edges of the action potentials, and proceed according to Eq. (5). Since this equation contains only a sum of parts of the $x(t)$-signal—taken at and around (or, prior to) the instants t_i at which $s(t)$ contains an impulse—the actual computation of the cross-correlation function is very simple indeed.

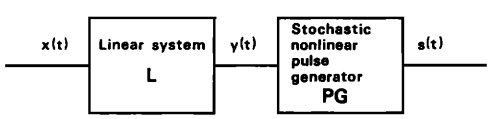

FIG. 2. Nonlinear frequency-selective pulse generating system, can be used as a model of a primary auditory neuron.[1]

FIG. 3. The network of Fig. 2 shown as a cascade of simpler devices.

The derivation presented above provides the general theory behind the method of reverse correlation as applied to the study of the cochlear encoding process. It should be noted that the method does not "exist" without a model: i.e., its result can only be expressed in terms of that model. In other words, the result of the experimental procedure, which comes in the form of an (unbiased) estimate of the revcor function, is nothing more than a parameter of the underlying model (Fig. 2). If the appropriate parameter is substituted, the model should provide an optimal match to the experimental observations. The validity of the model in a more general sense must be justified by an independent test. Such a test is described in Sec. II.

We now present some typical results of the application of the reverse-correlation procedure to responses recorded from auditory-nerve fibers. The experimental setup is schematized in Fig. 4. Anesthetized cats are used as experimental animals. The stimulus signal—white noise—$x(t)$ is presented by an earphone via a closed acoustic system. The (electrical) signal $x(t)$ is fed also to the computer (DEC PDP-9). From this moment on, the signal $x(t)$ assumes the role of the stimulus signal. Thus, the electroacoustical transfer function is absorbed in the linear system L of the model. Action potentials recorded from an auditory-nerve fiber are converted into pulses and sent to the computer via a digital channel. The procedure outlined in the previous paragraphs calls for processing of the stimulus signal $x(t)$ as guided by the occurrence of action potentials recorded. Since only negative values of τ are involved [cf. Eq. (2b)] the processing involves addition of stimulus signal fragments that occur prior to each action potential. To achieve this, the computer continuously reads in the x signal via its analog-to-digital system, so that the immediate past of $x(t)$ (over, e.g., 50 ms) is available every time an action potential is detected. It is to be noted that in an actual experiment only an estimate of the revcor function can be obtained, due to the limited time of observation. Appendix A gives more details about experimental and computational procedures, calibration, polarity conventions, etc.

Figures 5–8 show experimental results for four primary auditory neurons measured in cats. Figures 5(a), 6(a), 7(a), and 8(a) show the waveshapes of the revcor func-

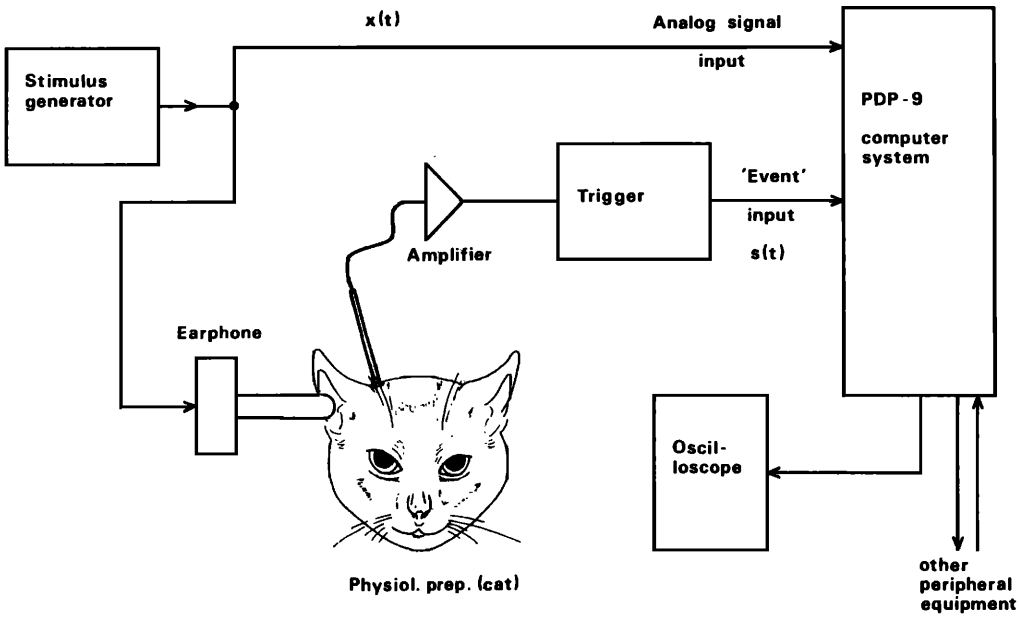

FIG. 4. Setup to measure a revcor function.

tions as they are obtained after the processing of more than 4000 action potentials. The functions are measured with white-noise stimuli presented at a level of 20–40 dB above the fiber's threshold, see the legends to the figures. Threshold is defined here as the acoustical level at which the presentation of a 50-ms burst of noise produces a just discernible increase in firing rate. The revcor functions show several oscillations with a fairly rapid build up and a tail of slowly decaying amplitude. The frequency of these oscillations corresponds to the characteristic frequency of the fiber. Hence we associate a resonance frequency with each revcor function, and we may identify this with the characteristic frequency (CF) of the fiber. The waveshapes reported in these figures are representative of the hundreds of revcor functions we obtained from cat experiments, with resonance frequencies ranging from 0.34 to 5 kHz. In general the relative bandwidth decreases with increasing resonance frequency. The variations are quite large, however; the neuron shown by Fig. 7, for instance, has a larger-than-average bandwidth.

All revcor functions show an initial delay; this delay not only reflects propagation time in the cochlea but also includes the buildup time of the action potential from its locus of initiation to the recording electrode. In the model of Fig. 3 the neural pulse generator is assumed to be an instantaneous device. Hence all delays show up as an initial delay in the recovered impulse response $h(t)$ for L. As mentioned before, the transmission characteristics of the electroacoustic system are absorbed in L too. As long as the same system is used, no correction is necessary for the comparison of responses to different stimuli.

Figures 5(b), 5(c), 6(b), 6(c), 7(b), 7(c), 8(b), and 8(c) show the "revcor spectra," i.e., the Fourier transforms of the revcor functions. The amplitude spectra [5(b), 6(b), 7(b), and 8(b)] are plotted on logarithmic scales and upside down so as to stress the resemblance to pure-tone tuning curves. The spectra are cut off at a distance of up to 40 dB from the top since components further away from the top are due to measurement inaccuracy. When plotted on logarithmic coordinates, these amplitude spectra are somewhat asymmetrical around their resonance frequencies. On a linear frequency scale, however, they appear as nearly symmetrical. The amplitude spectra of revcor functions have been reported to be quite similar to pure-tone tuning curves (de Boer, 1969a, 1973) in the region around the resonance frequency, albeit that the tuning curves may be somewhat steeper.

Figures 5(c), 6(c), 7(c), and 8(c) show the phase responses associated with the spectra. Two points are of interest here. First, the revcor function shows an initial delay and, as a consequence, the phase changes fairly rapidly as a function of frequency. To improve clarity, each phase value at a particular frequency is plotted as the *difference* of the actual phase and the phase due to a pure delay at the same frequency. The delay used for this correction is indicated in the figure. For reference purposes, the pure-delay phase is also shown (dotted). The second point is that the spectrum cannot be estimated accurately down to zero frequency and hence it is not possible to find out how many times a phase of 2π is accumulated. For this reason the phase at the resonance frequency is plotted as its true value between $-\pi$ and $+\pi$, and all phase values are plotted with respect to this reference point. The correction phase is taken as zero at this point. We observe that the phase responses are fairly regular throughout the resonance region.

The main source of error in the reverse-correlation procedure is finite sample size: Several thousands of action potentials are processed for each revcor function shown, yet random fluctuations are clearly visible. Under the assumption that errors are independent and additive, the experimental functions can be smoothed by removing from the waveform or the Fourier spectrum those components that appear to be entirely random.

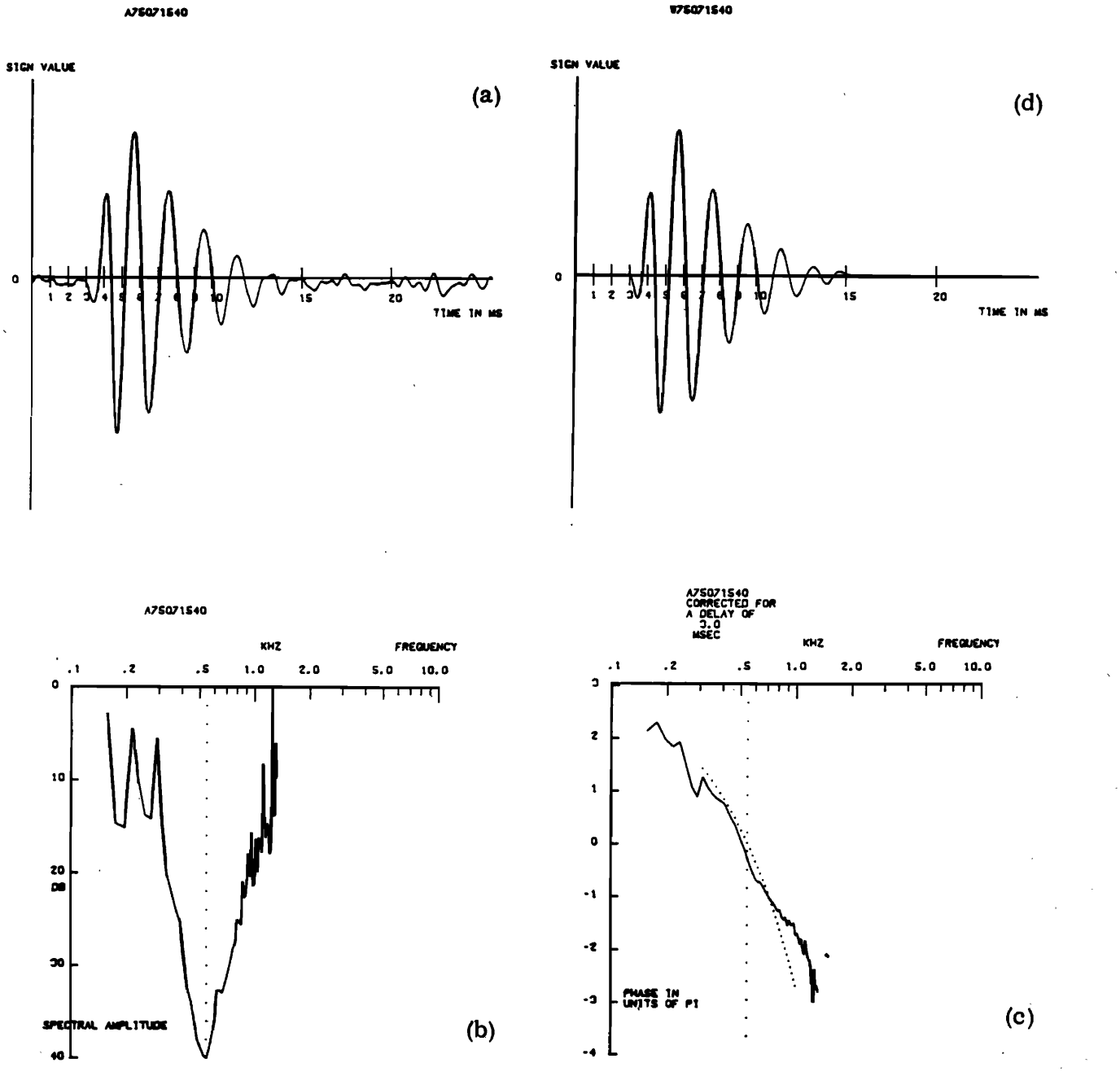

FIG. 5. Revcor function of unit 75-07-15, resonance frequency: 530 Hz, threshold for noise: 20 dB (SPL)/third oct., stimulation level: 40 dB/third oct. (a) Waveform of revcor function (vertical scale arbitrary). (b) Spectral magnitude (inverted). (c) Phase characteristic (see text). (d) Smoothed waveform.

The smoothing procedure is alternatingly carried out in the frequency and the time domain. Figures 5(a), 6(a), 7(a), and 8(a) of the figures show the raw data, Figs. 5(d), 6(d), 7(d), and 8(d) the smoothed revcor functions. Most of the characteristic features of the functions are preserved. The smoothed versions of the revcor functions are convenient for further analysis of stimulus-response relationships, see Sec. II.

In view of the linearizing tendencies of correlation methods, separate tests are necessary to assess the part played by cochlear nonlinearity. One impression of nonlinearity can be obtained by measuring via the reverse-correlation technique whether frequency selectivity of a neuron is dependent upon stimulus intensity. For low-to-moderate levels of stimulation, the revcor functions are found to be almost invariant. The largest variations occur in the phase response, they appear as a uniform phase shift limited to $\pi/4$ rad. At levels of over 70 dB SPL per $\frac{1}{3}$ octave (83 dB SPL overall level for a bandwidth of 5 kHz) some revcor functions change their appearance. In terms of the waveform an increased damping is evident. In terms of the spectrum, the relative bandwidth becomes broader with increasing level and the top shifts to a lower frequency. This behavior is reminiscent of the nonlinearity in mechanical tuning that was reported by Rhode (1971). We did not find this behavior, however, in all fibers tested at high

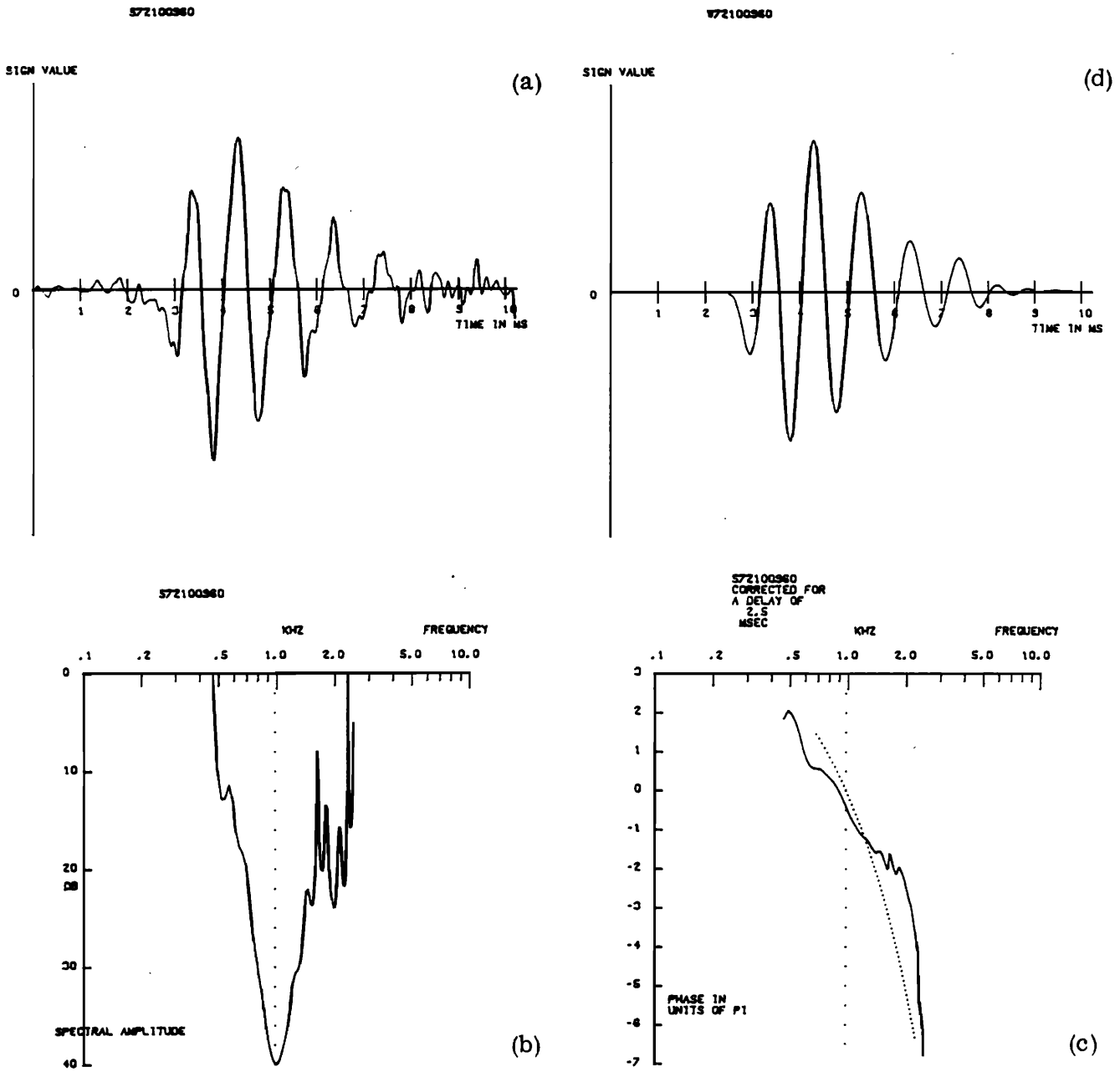

FIG. 6. Revcor function of unit 72-10-09, resonance frequency: 1 kHz, threshold for noise: 30 dB/third oct., stimulation level: 60 dB/third oct.

intensities. Comparable results on properties of revcor functions were recently reported by Evans (1976, 1977). A possible explanation for these findings will be described in the discussion. Further experiments that give an indication as to how important cochlear nonlinearity is in signal processing are presented in the next section.

II. VERIFICATION (SIMULATION PROCEDURE)

The experiments described in the present section are designed to test the predictive power of the model underlying the reverse-correlation procedure. The principal idea is to measure the revcor function for a primary auditory neuron, to substitute this function as the impulse response in the model of Fig. 2 and to compare the timing pattern of actual nerve firings with predictions from the model. If the model holds true, the firing probability $p(t)$ of the neuron should be a monotonic function of the output $y(t)$ of the linear filter L. We will presently see to what extent $y(t)$ is a good predictor of $p(t)$. The procedure is called the *simulation procedure* (cf. de Boer and de Jongh, 1971; de Jongh, 1972, 1973; Grashuis, 1974). In the present report the emphasis will be on the accuracy of timing prediction and the evidence of specific nonlinear effects.

Figure 9 shows a flow diagram of the simulation procedure. First, the revcor function of the nerve fiber under study is determined, using white noise as the stimulus [Fig. 9(a)]. In smoothed form this revcor function—to be called $h^*(t)$—is substituted as the impulse response of the model filter L^* (an asterisk denoting

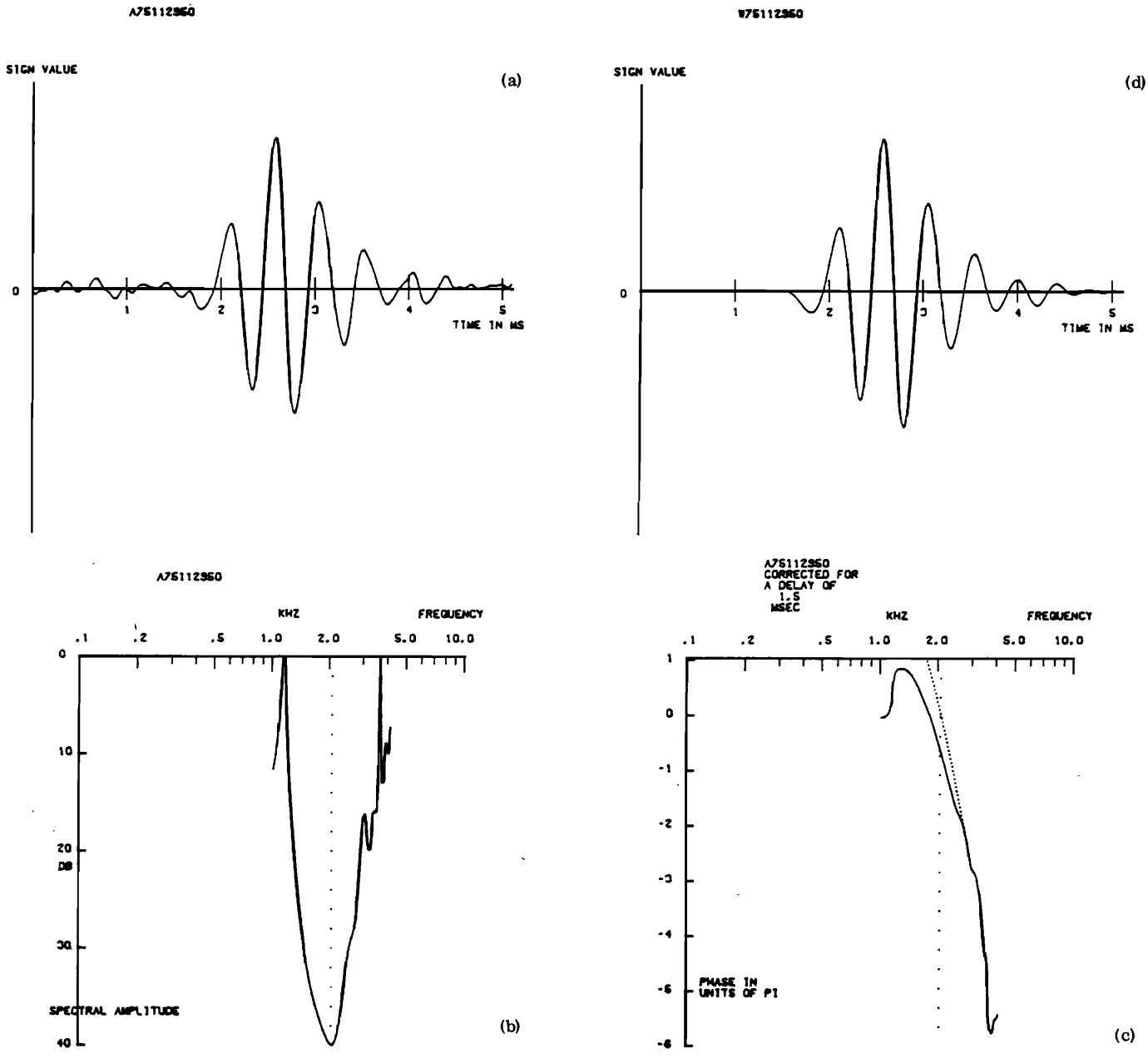

FIG. 7. Revcor function of unit 75-11-29, resonance frequency: 2.1 kHz, threshold for noise: 20 dB/third oct., stimulation level: 50 dB/third oct.

the fact that the quantities and concepts involved are based on a statistical estimate of the revcor function). In the second stage [Fig. 9(b)] a new stimulus signal $x(t)$ is generated which is periodic with the period T; this signal $x(t)$ is led to the animal's ear as well as to the input of the filter L^*. The firing probability $p(t)$ of the (same) nerve fiber is determined from the physiological preparation in the form of a PST histogram of the nerve firings over the interval T. The response $y^*(t)$ of the filter L^* is computed according to the well-known convolution theorem. The signal $y(t)$—of which we can only measure its estimate $y^*(t)$—is called the excitatory signal. It should be noted that the excitatory signal is used in the physical (and not in the physiological) sense: It is just a filtered form of the stimulus $x(t)$ and nothing else.

The first case to be described is that of stimulation with repetitive noise (pseudorandom noise). After the revcor function of a primary neuron was determined with truly random noise, the same neuron was stimulated continuously by presenting pseudorandom periodic Gaussian noise generated by the Hewlett Packard noise generator type 3722 A. The bandwidth of the noise was 5 kHz and the period of repetition 0.082 s ($N=13$); the uppermost panel of Fig. 10(a) shows the noise waveform. The PDP-9 computer was programmed to accumulate a PST histogram of the nerve firings with the onset of the noise repetitions as the zero point for time. The lowest panels of Fig. 10(a) show parts of the measured PST histogram, i.e., the function $p(t)$, together with the computed waveform of the filter output $y^*(t)$. For the computation of $y^*(t)$ a smoothed version $h^*(t)$ of

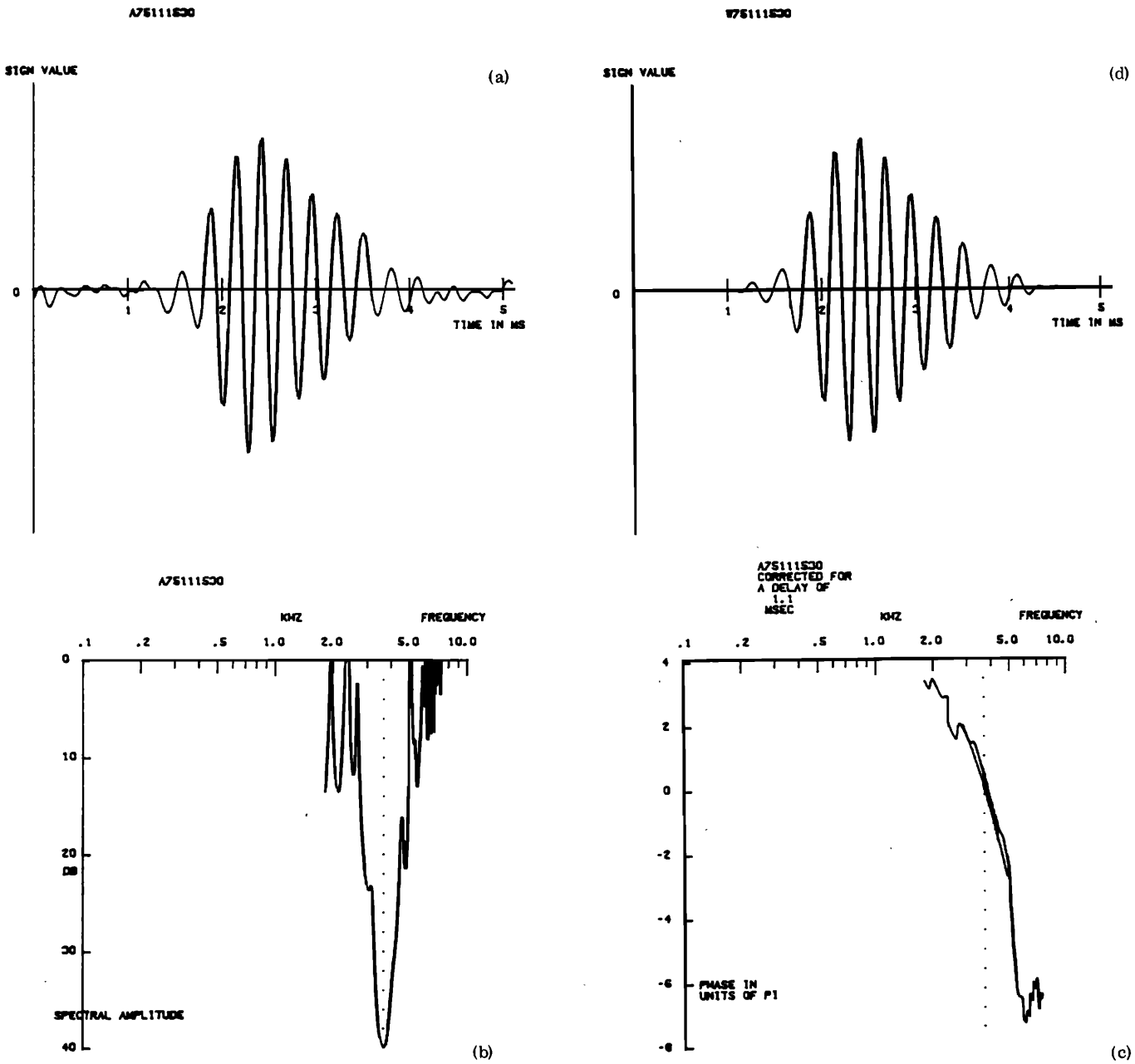

FIG. 8. Revcor function of unit 75-11-15, resonance frequency: 4.66 kHz, threshold for noise: 10 dB/third oct. stimulation level: 30 dB/third oct.

the revcor function was used, see the inset of this figure. The amplitude scales for $y^*(t)$ and $p(t)$ are arbitrary.

The neuron under study (75-08-73) had a resonance frequency (CF) of 800 Hz. It is evident that $y^*(t)$ predicts the time course of the probability of firing $p(t)$ to a large degree. For positive values of $y^*(t)$, the average relation between $p(t)$ and $y^*(t)$ appears to be nearly linear. For negative values of $y^*(t)$, the probability of firing is practically zero. Figures 10(b) and 10(c) show further examples of measured $p(t)$ and computed $y^*(t)$ signals for two other neurons with low resonance frequencies, 1.2 and 2.1 kHz, respectively. The stimulus was the same repetitive noise signal. In Fig. 10(b) we note that the largest positive values of $y^*(t)$ do not give rise to a fully proportional $p(t)$. In Fig. 10(c) we note just the opposite: The smaller excusions of $y^*(t)$ seem to produce a disproportionally small number of spikes. It is as if the neuron has an "instantaneous threshold," i.e., when $y^*(t)$ is below a certain (positive) level, the neuron is not likely to fire. Still, the actual threshold of this neuron is lower, see Fig. 7. We may conclude that the relation between $y^*(t)$ and $p(t)$ appears to be nearly monotonic but its character varies from neuron to neuron. There is another interesting feature in Fig. 10(c): In the smaller excursions of $y^*(t)$ we observe a small shift in timing of the firings. It is as if a certain phase modulation is present in these periods. It is probable that errors in the estimation of the revcor function $h^*(t)$ produce time shifts of $y^*(t)$; it is also probable, however, that this effect is a manifestation

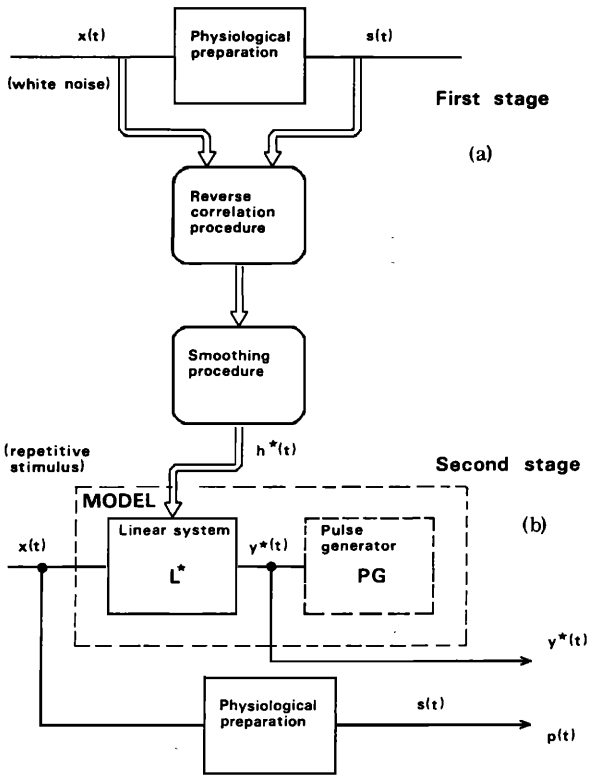

FIG. 9. Illustrating the stages of the simulation method. See text. In the first stage the revcor function is measured and processed. The stimulus is white noise. In the second stage the response of the (same) physiological preparation is compared with the response of the linearized model. The stimulus is a repetitive signal in this stage.

of nonlinearity. We will come back to this later.

There are small but systematic differences in waveshape between $y^*(t)$ and $p(t)$. These differences are larger for neurons with a higher resonance frequency. Figure 11 presents the result of the simulation procedure for a neuron with a resonance frequency of 2.6 kHz. Again the firing probability $p(t)$ is nearly a rectified version of $y^*(t)$. For this fiber, however, the individual lobes of the $p(t)$ function are asymmetrical. Their left-hand flanks are steep, and their right-hand flanks are shallower and have a tendency for "crossing over" to the next lobe. This is not a result of processing or measurement errors but, quite likely, reflects intermediate steps in the initiation of nerve impulses that are not accounted for by the simple model of Fig. 2 and that show up more clearly when the resonance frequency is high. For primary auditory neurons with still higher resonance frequencies this tendency is more pronounced and the firing probability ceases to follow every lobe of $y^*(t)$. In a certain sense, the firing probability tends to be controlled by the envelope of the $y^*(t)$ signal. Figure 12 shows the result for a neuron with a resonance frequency of 4.7 kHz, an extreme case that serves well to illustrate this point. Note the enlarged time scale in this figure. We observe here a manifestation of the same cause that prevents us from measuring revcor functions in neurons with resonance frequencies above 6 kHz.

Up to now we have processed the records of 31 neurons in this way. In all we found the same type of result. We conclude that for the type of stimulus used, repetitive wide-band noise, the model of Fig. 2 produces an adequate prediction of the firing probability. The main correction that should be applied concerns the observed skewness of the $p(t)$ lobes as shown in Figs. 11 and 12 (cf. also Fig. 14). In any event, the reverse correlation function (revcor function) provides the main parameter, the impulse response function $h^*(\tau)$, of the model. It is recalled that the revcor amplitude spectrum around its top approximately coincides with the tuning curve (de Boer, 1973). It appears, then, that the revcor function describes several aspects of tuning: the tuning for pure tones around the CF and the time course of the response to (pseudo-) random wide-band noise. The predictions of the model hold true over the range of fluctuations in $y^*(t)$ such as are encountered with a stationary noise stimulus. The results presented apply to the case of stimulation with levels of up to 30–40 dB above threshold. We found the same type of result under conditions where the neuron saturates. Within each lobe of $y^*(t)$ only a slight flattening of $p(t)$ occurs near its maxima [note that the neuron of Fig. 10(b) was not saturated]. The same applies to the case of stimulation at intensities of over 70 dB SPL per third octave. Here we obtain the best results when we use a revcor function that is measured with the same level of stimulation. These remarks are meant to be of a descriptive nature; we have processed too few recordings made under these conditions to be more specific.

Cochlear nonlinearity is so pronounced that under specific circumstances, responses occur to distortion products (the cubic difference tone, in particular) and *not* to the primary components generating these distortion products (Goldstein and Kiang, 1968). Similarly, two-tone suppression can occur by tones that are below threshold (e.g., Sachs and Kiang, 1968). In these respects, nonlinearity seems to override cochlear frequency selectivity. We may expect components outside the passband of the system to affect the transmission of components inside the passband. This is a reason to pay attention to effects that betray the influence of nonlinear filtering. Those effects occur in the phase and amplitude modulations that are inherent in narrow-band noise signals (de Boer, 1976b). With this in mind, we turn again to Figs. 10–12 and observe that there are no obvious phase deviations between $y^*(t)$ and $p(t)$ [except for the slight effect in Fig. 10(c)]. In general terms, nonlinear filtering in the cochlea, however strong it may be, seems to leave no trace in the response to wide-band stimuli such as pseudorandom noise. See the next section for a further analysis.

All this applies to stationary stimuli. The next question is: What happens in the case of nonstationary stimuli? For the results shown by Fig. 13 a toneburst of 50-ms duration was presented periodically with a period of 0.1 s. The tone was switched on and off with zero rise time (the uppermost trace shows the stimulus waveform). It is seen from the central trace that the preferred cycles of firing as well as the cycles of suppression are cor-

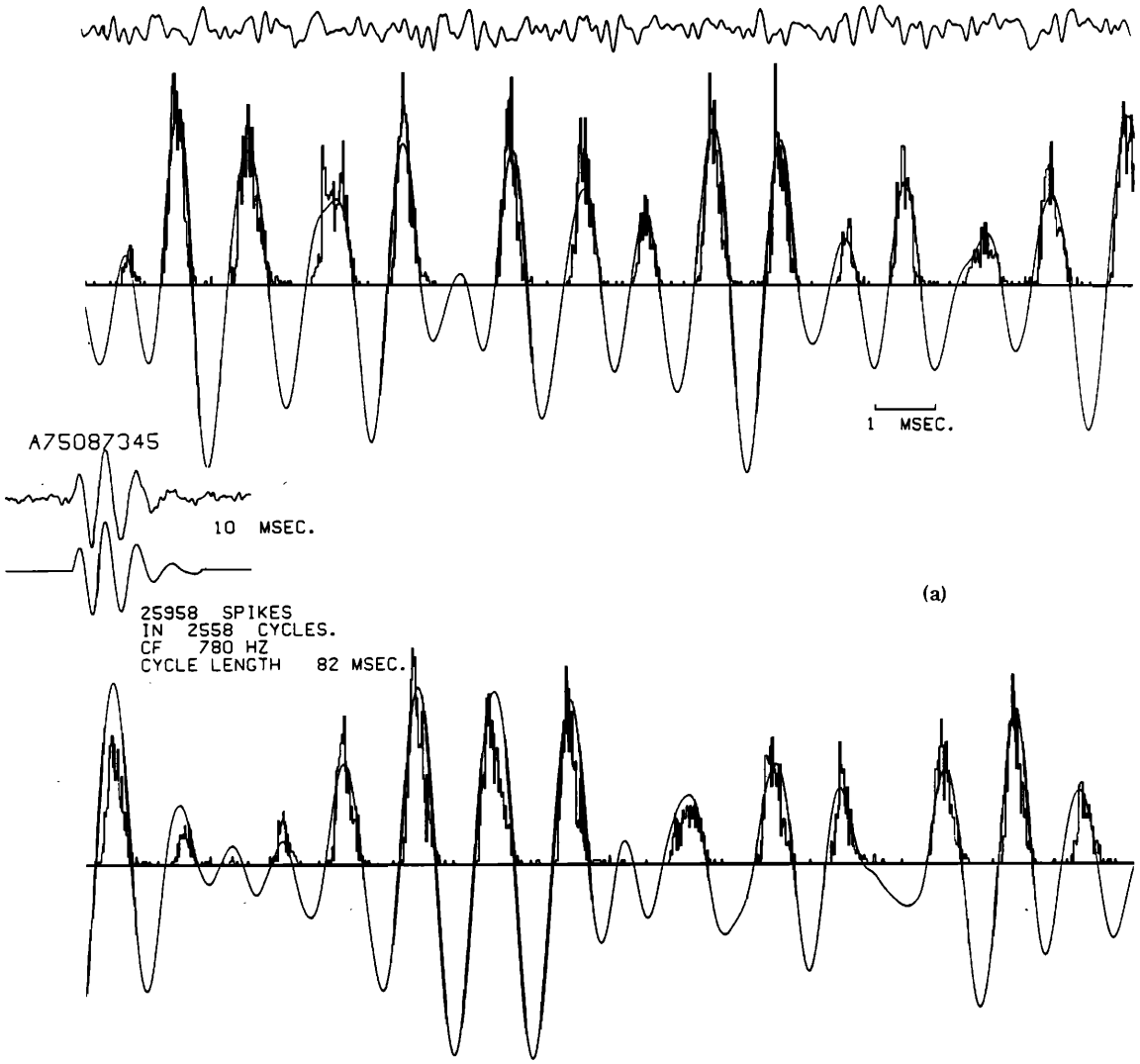

FIG. 10(a). Results of the simulation method for unit nr.: 75-08-73, resonance frequency: 0.780 kHz, stimulation level: 45 dB/$\frac{1}{3}$ oct. The upper trace shows the stimulus waveform $x(t)$; the other traces show the computed $y^*(t)$ signal (smooth line) and the measured $p(t)$ function (as a histogram). The lower panel shows a different part of the recording. The inset shows the revcor function, in both raw and smoothed forms. The latter version is used as $h^*(t)$ to compute $y^*(t)$. The unit, as are those in Figs. 10(b) and 10(c), is stimulated at 30 dB above its threshold for noise.

rectly predicted by the (linear) model. Even during the buildup phase of the $y^*(t)$ response, there is no trace of a decrease or a change of synchronization. However, in the first few cycles of $y^*(t)$ the firing probability $p(t)$ is far larger than in later cycles; this is the manifestation of adaptation as it occurs during the onset phase. The lowest panel of this figure shows the response to the sudden cessation of the stimulus. Again it is seen that the linear response $y^*(t)$ correctly predicts the lobes of the histogram but in this case the amplitudes of the $p(t)$ lobes decay more slowly than those of $y^*(t)$—this is probably another manifestation of the adaptation process. Finally, it should be noted that the "after oscillations" in the firing probability, after the cessation of the stimulus, occur with the resonance frequency, just as is the case of $y^*(t)$.

We did not explore stimulation with pure tones in a systematic way. We satisfied ourselves by noting that the average phase of the response to tones presented at up to 20 dB above threshold corresponds (within, say, 30°) to the phase of the revcor function at the corresponding frequencies. This comparison was done while measuring tuning curves and was found to hold over the frequency range over which the definition of the revcor phase spectrum is meaningful.

Figure 14 presents the result of the simulation procedure when a suddenly starting noise burst is used as the stimulus. In each panel the upper trace shows the stimulus waveform, the other traces the signals $y^*(t)$ and $p(t)$. In this case the burst was chosen long enough (82 ms) to permit observation of the onset transient [Fig. 14(a)] as well as the steady-state behavior [Fig. 14(b)]. In Fig. 14(a) the gradual building up of the $y^*(t)$ waveform, reflecting the resonance implicit in the revcor

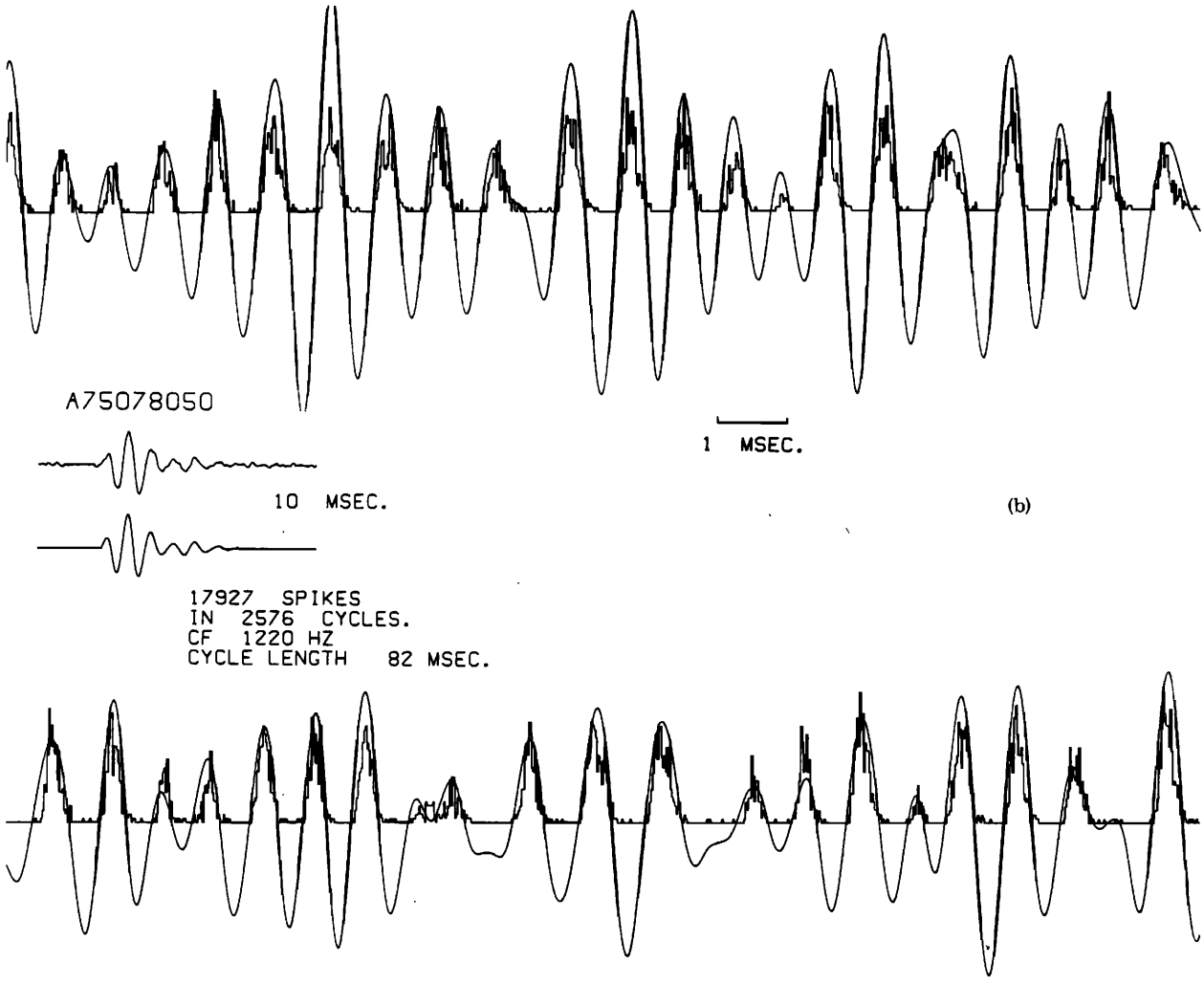

FIG. 10(b). Same as Fig. 10(a), but for unit nr.: 75-07-08, resonance frequency: 1.22 kHz, stimulation level: 50 dB/$\frac{1}{3}$ oct. The stimulus waveform is omitted.

function, is recognized. The firing probability appears to follow $y^*(t)$ closely but its initial amplitude is far larger than in later sections of the signal. There is no apparent distortion of the amplitude and phase modulations of the signal. From the instant marked by a dashed vertical line on, the waveform of the stimulus in Fig. 14(a) is identical to that in Fig. 14(b). Apart from the aforementioned difference in amplitude, the waveforms of $p(t)$ in these two parts are found to be practically identical. We observe again the tendency for "overlapping" between the individual lobes of $p(t)$ that was mentioned in connection with Fig. 11.

This figure, then, confirms that for a wide-band noise stimulus a linear transform of the stimulus is the prime controller of firing probability. Of the nonlinear effects only short-term adaptation is manifest, it appears as a multiplicative effect, modulating the firing probability when sudden changes in stimulus occur, and reducing firing probability as the stimulus continues. Note that the first phase of adaptation is very fast, it is almost completed within 2 ms. It is remarkable that fast adaptation shows up only in the form of onset and offset effects. In the course of the response to a stochastic signal there occur many fluctuations in the excitatory signal $y^*(t)$, but short periods in which the oscillations have a nearly constant amplitude occur as well. We do not observe systematic adaptation effects during these periods. Apparently, fast adaptation shows up only when the amplitude changes rapidly over a wide range.

III. AUTOCORRELATION ANALYSIS

Of the many nonlinear effects in the cochlea, we want to pay particular attention to nonlinear filtering. The recordings presented so far do not betray much evidence of a derangement of filtering due to nonlinear effects. On the contrary, the results confirm that a linear transform of the stimulus signal is the prime controller of firing probability. This holds true within the following constraints: the application of wide-band stochastic stimuli or single pure tones in the main passband, and the use of stimuli with constant (average) intensity. In this section we subject the results to further analysis with the aim to detect possible effects of nonlinear filtering of a more subtle nature. In particular, we want to determine the fine structure of the spectrum of the $p(t)$ function for noise excitation. As said earlier, nonlinear filtering is most likely to affect the relation between intrinsic amplitude and phase modulation of signals

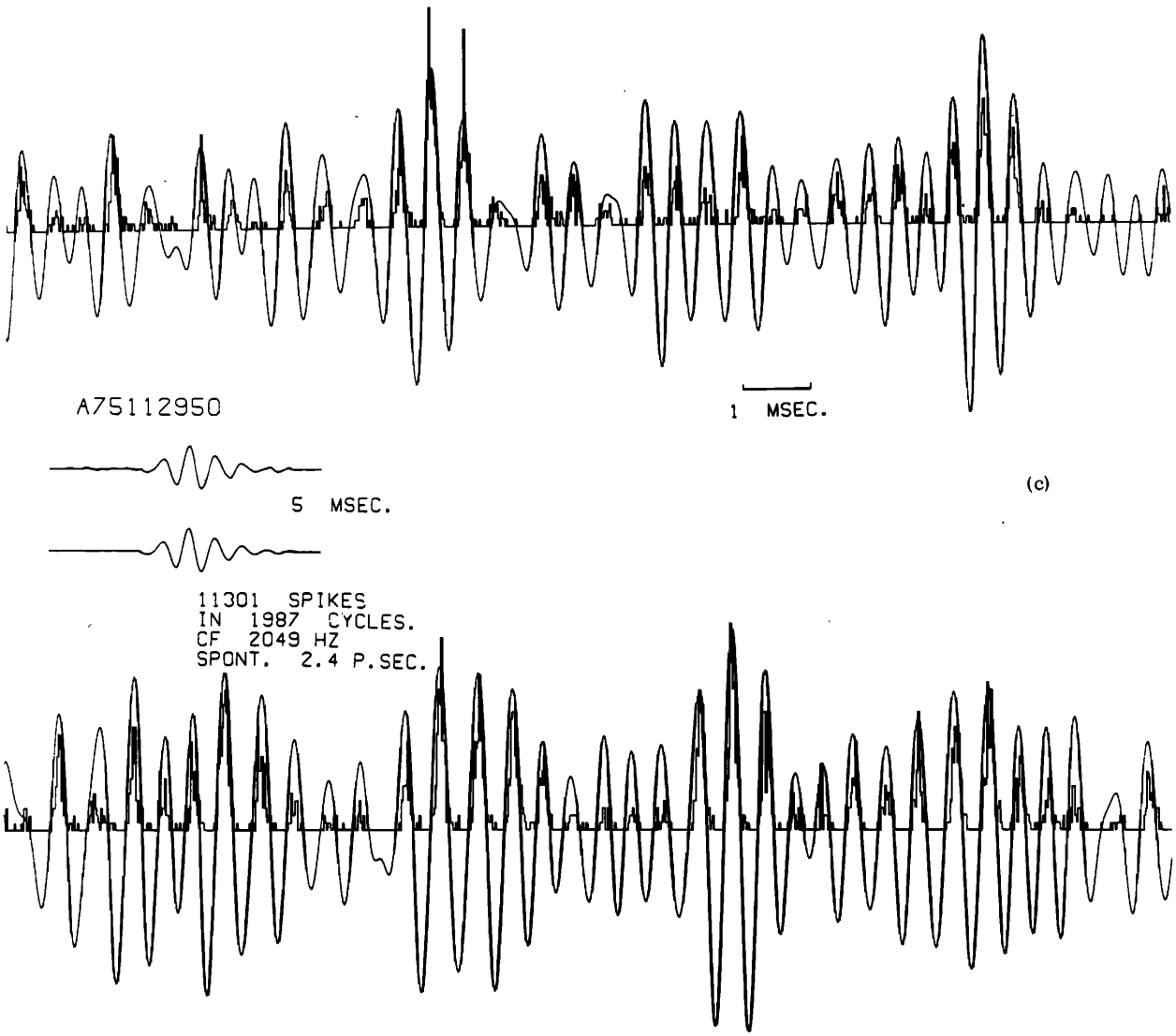

FIG. 10(c). Same as Fig. 10(a), but for unit nr.: 75-11-29, resonance frequency: 2.05 kHz, stimulation level: 50 dB/$\frac{1}{3}$ oct. The stimulus waveform is omitted.

(de Boer, 1976b) and this should be evident in the form of a modification of the spectrum. To this aim we first compute the autocorrelation function (acf) $\psi_p(\tau)$ of $p(t)$ and compare this with the acf $\psi_y(\tau)$ of $y(t)$. (For reasons of clarity we leave out the asterisks here.) The comparison will be executed in the frequency domain on the basis of the power spectra $\Psi_p(\omega)$ and $\Psi_y(\omega)$ corresponding to these functions.

The processing of the computed $y(t)$ signal presents no difficulties. In the processing of experimental $p(t)$ functions, however, we have to correct for two (trivial) types of nonlinearity. The most important one of these is rectification: The firing probability $p(t)$ is a nonnegative function of time. In Appendix B it is described how it is possible to correct for rectification. In essence, the acf computed from the measured $p(t)$ function is predistorted so that an acf $\psi_q(\tau)$ is obtained that corresponds to a Gaussian variable $q(t)$ which is identical to $p(t)$ whenever the latter is positive. This transformation of the acf is called "derectification." Consequently, when we refer to the power spectrum $\Psi_p(\omega)$ we actually mean $\Psi_q(\omega)$. The only proviso is that $p(t)$ is assumed to have the probability distribution of a rectified Gaussian variable. As it turns out, the effect of "derectification" on the main part of $\Psi_p(\omega)$ is very small indeed. (In effect we measured and processed some functions $p(t)$ in the form of a "compound histogram" as originated by Pfeiffer—see, e.g., Goblick and Pfeiffer (1969)—but this was found to be an unnecessary complication for the present purpose.) Thus the condition is not a very stringent one.

The second trivial type of nonlinearity concerns the form of the (instantaneous) relation between $y(t)$ and $p(t)$. See the remarks made in connection with Figs. 10(a)–10(c). Since derectification has so little effect on the shape of $\Psi_p(\omega)$ in the main frequency band, further corrections of instantaneous nonlinearities are not necessary (cf. Davenport and Root, 1958). Further details of data processing are given in Appendix B.

Figure 15(a) shows the result of this procedure applied to the $p(t)$ function of the neuron of Fig. 10(a). The figure

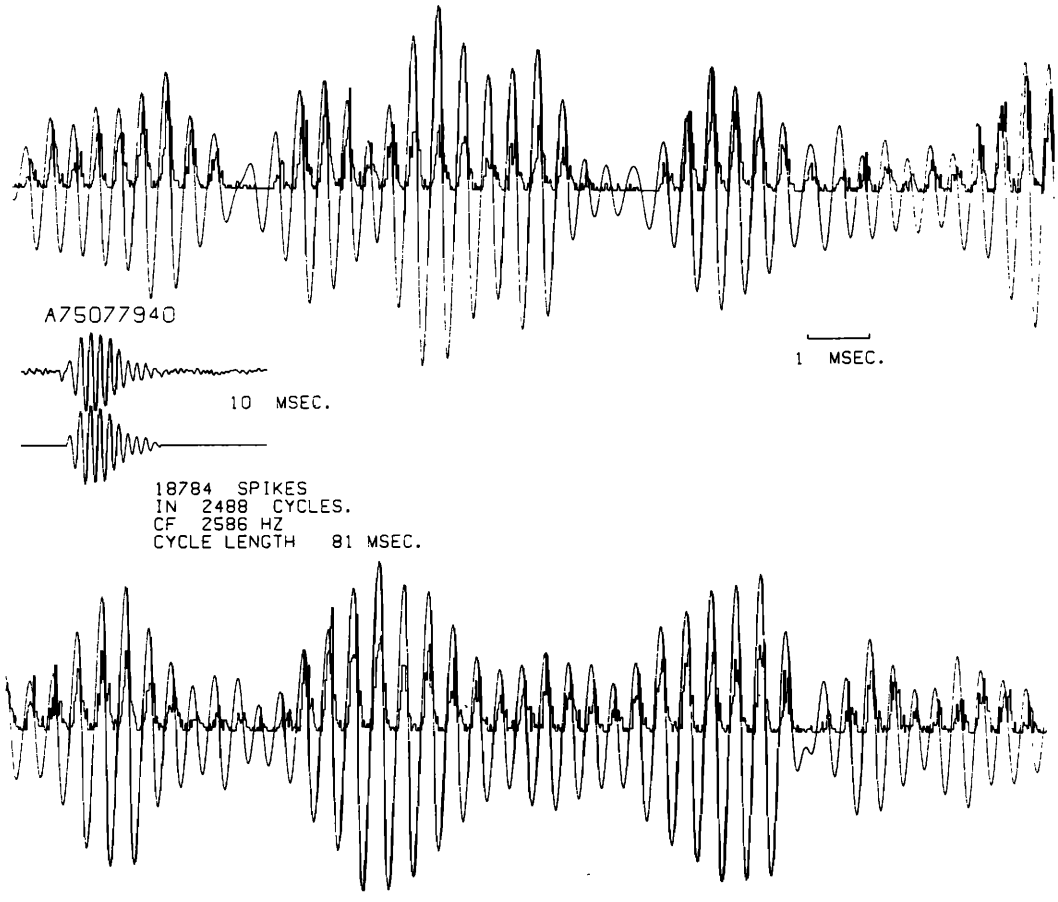

FIG. 11. Same as Fig. 10 but for a neuron with a higher resonance frequency. Unit nr.: 75-07-79, resonance frequency: 2.6 kHz, stimulation level: 40 dB/third oct.

shows the power spectra in much the same way as Figs. 5(b)–8(b) but the frequency scale is widened considerably. Three spectra are shown; below, the one corresponding to the measured $p(t)$ function [actually $q(t)$], center, the one corresponding to the $y(t)$ function, the third one (top) being the power spectrum belonging to the acf computed from the revcor function $h(t)$. The three spectra are, for reasons of clarity, displaced over 5 dB with respect to one another. The latter two spectra should be identical when the input signal is (true) white noise; any remaining differences are to be attributed to processing effects, and, more important, to the fact that $\psi_y(\tau)$ is computed from a finite sample of a nonstochastic signal. As seen from the figure, the differences between these two spectra are less than 1 dB and can, therefore, be neglected. The third spectrum, that of $\psi_p(\tau)$ (actually, that of the corresponding q function) is very similar to the other two. The deviations are less than 1 dB over a range of 15 dB and may well be attributed to processing effects and sampling errors. We conclude that in this recording nonlinear filtering has not left any observable effect in the distribution of spectral components as they are represented in the firing pattern of the neuron. In particular, there is no widening of the resonance peak. This conclusion is corroborated by the results shown in Fig. 15(b) for another neuron with a fairly low resonance frequency, 1.5 kHz. It is seen that the p spectrum begins to be somewhat wider at a distance of more than 12 dB from the top. This may be caused by nonlinear effects (but this is by no means certain). We found the same type of results in ten other neurons with low resonance frequencies, with one exception. The deviations amount to 2 dB in this case and cannot be ascribed to processing errors.

Neurons with resonance frequencies well above 2.0 kHz show $p(t)$ functions that are definitely asymmetrical and tend to be more related to the envelope of $y(t)$ than to $y(t)$ itself, see Figs. 11 and 12. The autocorrelation functions $\psi_p(\tau)$ for such neurons reflect this aspect, of course. In fact they show an important component related to the acf of this envelope. But apart from this, $\psi_p(\tau)$ still reflects individual lobes of the $p(t)$ function and it is well possible to compare the spectra $\Psi_p(\omega)$ and $\Psi_y(\omega)$ in the region of resonance. Figure 16(a) shows the result of the processing of the data of the neuron of Fig. 14 of which the resonance frequency is 3.7 kHz. For this figure a still wider frequency scale was chosen in view of the small bandwidth involved. It appears that processing errors are somewhat larger but the result is consistent with the conclusion drawn above. Figure 16(b), finally, shows the result for the neuron of Fig. 12 with a resonance frequency of 4.7 kHz. For this neuron $\psi_p(\tau)$ shows only a small contribution related to the individual lobes of $y(t)$. With exactly the same processing it appears possible to study details of the representation

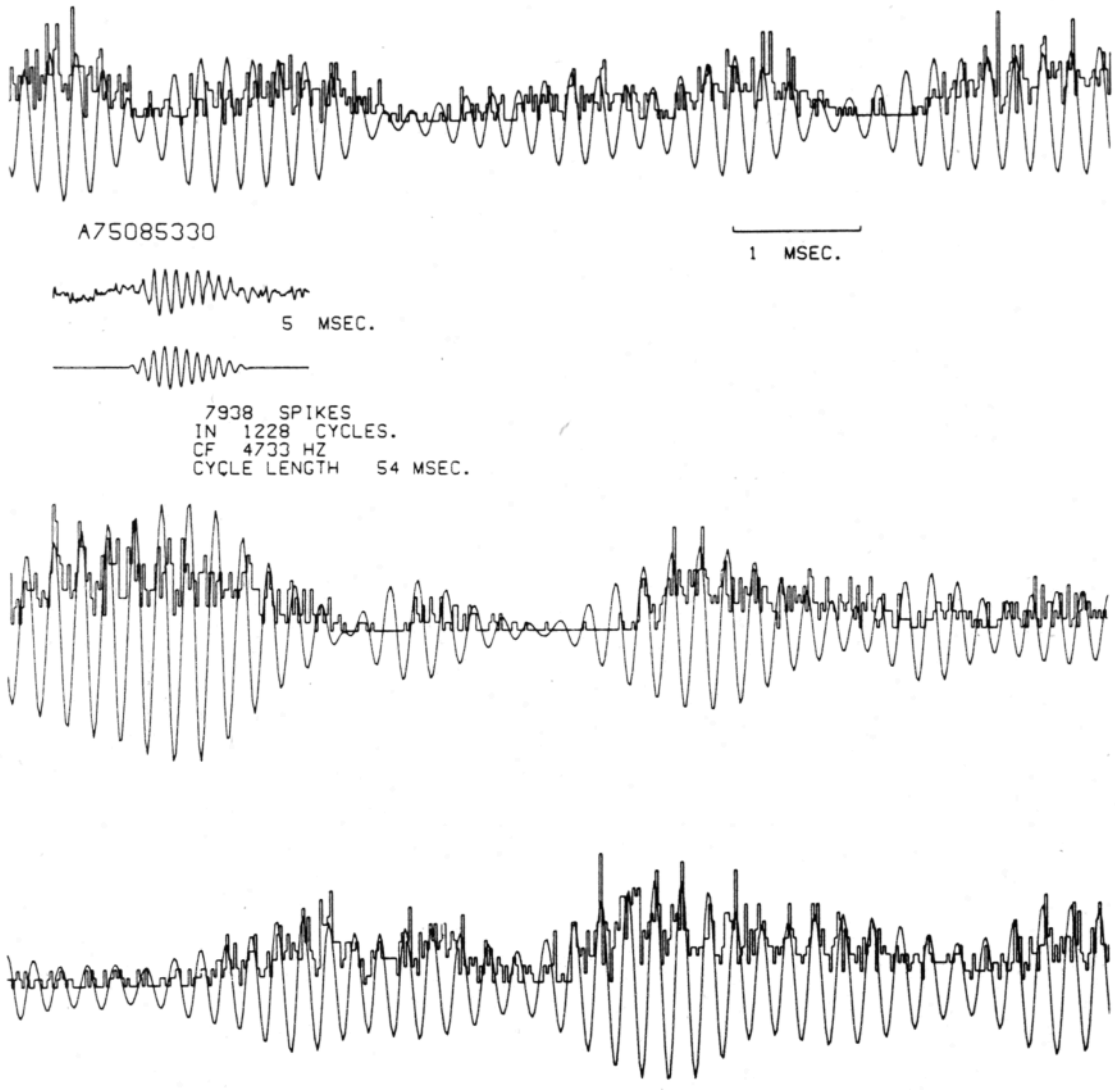

FIG. 12. Same as Fig. 10, for a neuron with a high resonance frequency. Unit nr.: 75-08-53, resonance frequency: 4.7 kHz, stimulus level: 30 dB/third oct. (20 dB above threshold), noise bandwidth: 15 kHz.

of frequency components in this neuron. The figure shows, then, that the spectrum $\Psi_p(\omega)$ in the passband is slightly wider than the spectrum $\Psi_y(\omega)$ but the slopes of the responses down from the resonance region are the same. Again we note that the effects of nonlinear filtering on the distribution of frequencies are marginal, if at all present. In quite general terms, cochlear nonlinearity (nonlinear filtering) is of such a nature that it does not noticeably affect the timing pattern insofar as this represents components in the frequency region of resonance. Nonlinear effects do show up in the form of fast adaptation and in the intensity dependence of revcor functions but neither of these two effects involves impairment of cochlear filtering. It should be remembered that this holds true for wide-band stimuli and for single pure tones.

IV. DISCUSSION

The reverse-correlation method is observed to yield a characteristic function representing fundamental aspects of the stimulus-response relation of a primary auditory neuron. This function turns out to be useful also for the prediction of firing patterns. In this respect the revcor function has advantages over conventional descriptors of the response pattern observed in auditory-nerve fibers, like the tuning curve or the click PST histogram. The method of reverse correlation has the additional advantage that it reveals details of frequency selectivity around the resonance frequency which are difficult to get otherwise. However, the method is not suited to reveal details about the skirts of the frequency response curve far from the top. In particular, the resolving power is not sufficient to assess the presence or absence of the low-frequency "tails" of the tuning curve in the revcor spectrum (cf. Kiang and Moxon, 1974).

All revcor functions have the general characteristics of the impulse response of a bandpass filter. We recall that the shapes of the revcor function's spectrum and the pure-tone tuning curve for the same fiber are most similar (de Boer, 1969a, 1973). General determinants of experimental revcor functions like initial delay, effective bandwidth, and slope of the spectrum are in good

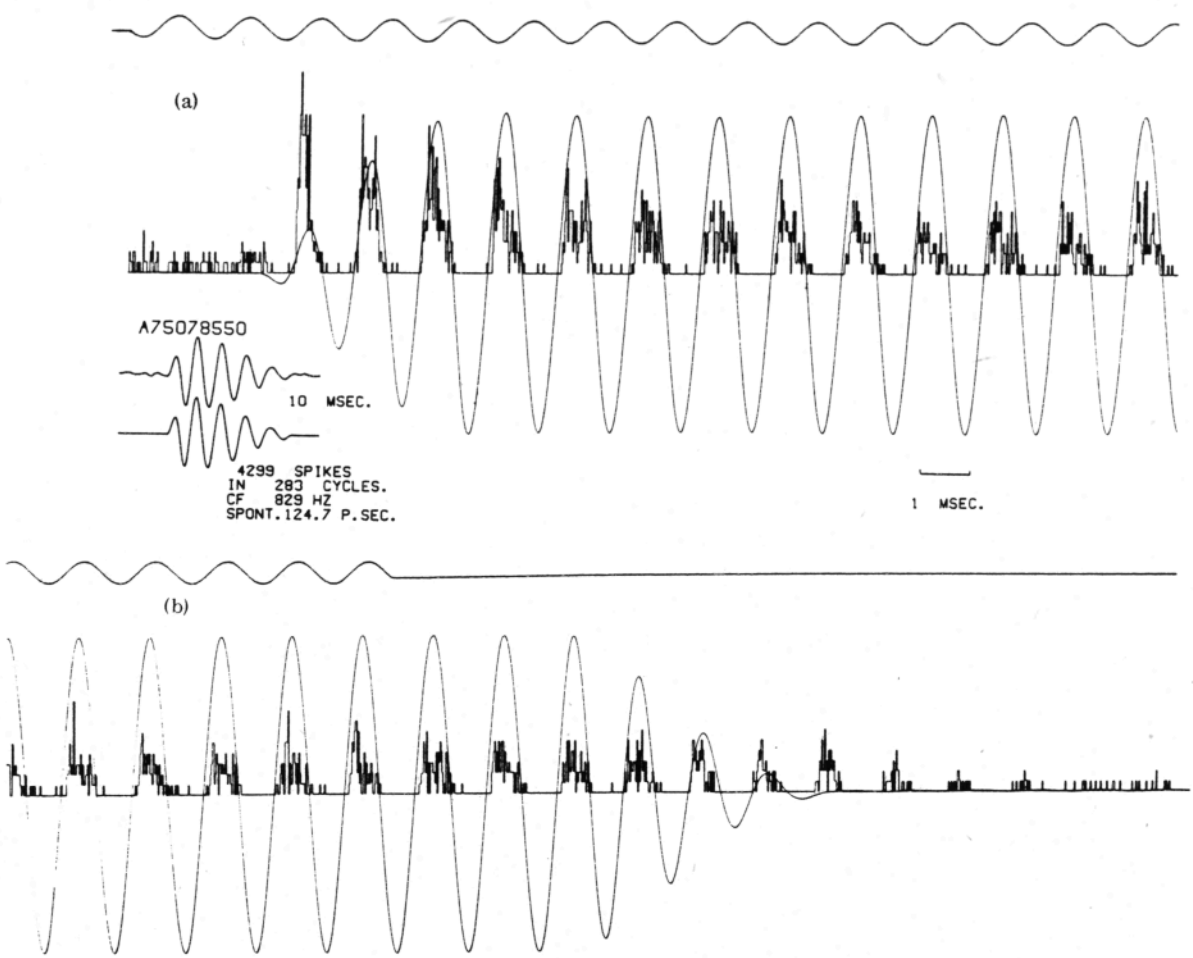

FIG. 13. Simulation result for a tone burst (a) shows the starting phase, and (b) the final phase. The layout is similar to that of Fig. 10(a). Unit nr.: 75-07-85, resonance frequency: 829 Hz, threshold at CF: 30 dB, stimulation frequency: 730 Hz, stimulus level: 50 dB.

agreement with corresponding data obtained by conventional methods (click PST histograms and pure-tone tuning curves). On a logarithmic frequency scale the amplitude spectra appear as asymmetrical. Mechanical response curves (e.g., Rhode, 1971) are highly asymmetrical. This difference suggests that a (second) filtering action is interspersed between mechanical events and excitation of the primary neuron (cf. Evans, 1972; Wilson and Evans, 1971). The phase characteristic of a revcor function shows around the resonance frequency a behavior that is reminiscent of a single resonating system. If we correct for the intrinsic delay (latency), the phase appears as an antisymmetrical function around the resonance frequency. The only rapid and asymmetrical phase changes occur at frequencies for which the spectral amplitude is more than 20 dB below maximum. The influence of these phase changes on the response pattern to wide-band stimuli is negligible.

Revcor functions have little or no phase modulation in the waveform. Evidence on the presence or absence of phase modulation in the mechanical response of the cochlea is conflicting. On the one hand, a clear break in the phase function near the point of resonance (Rhode, 1971) and a clear frequency modulation in the impulse response (Rhode and Robles, 1974) are reported from measurements with the Mössbauer effect. On the other hand, no evidence on phase modulation was obtained with the capacitive-probe method (Wilson and Johnstone, 1972). Again, if we consider cochlear frequency selectivity as a two-stage process, we are led to conclude that the second filter is much more selective than the first so that in the narrow range of resonance the break in the phase curve can no longer be observed. On the other hand, if sharpening is achieved by a simple transformation of the output of the mechanical filter (Hall, 1977; Allen, 1977), the latter conclusion holds true as well.

The results presented in Sec. II illustrate the predictive power of the revcor function and confirm the validity of the associated simple linear model. The acoustical signal $x(t)$, when it is filtered by an appropriate filter, produces a signal $y(t)$ that clearly delineates the periods of preferred firing and predicts the course of the firing probability in several details. This property holds true for wide-band stimuli, the predictions of the linear model are valid over the range of intrinsic variations in a stationary random stimulus. For slow variations

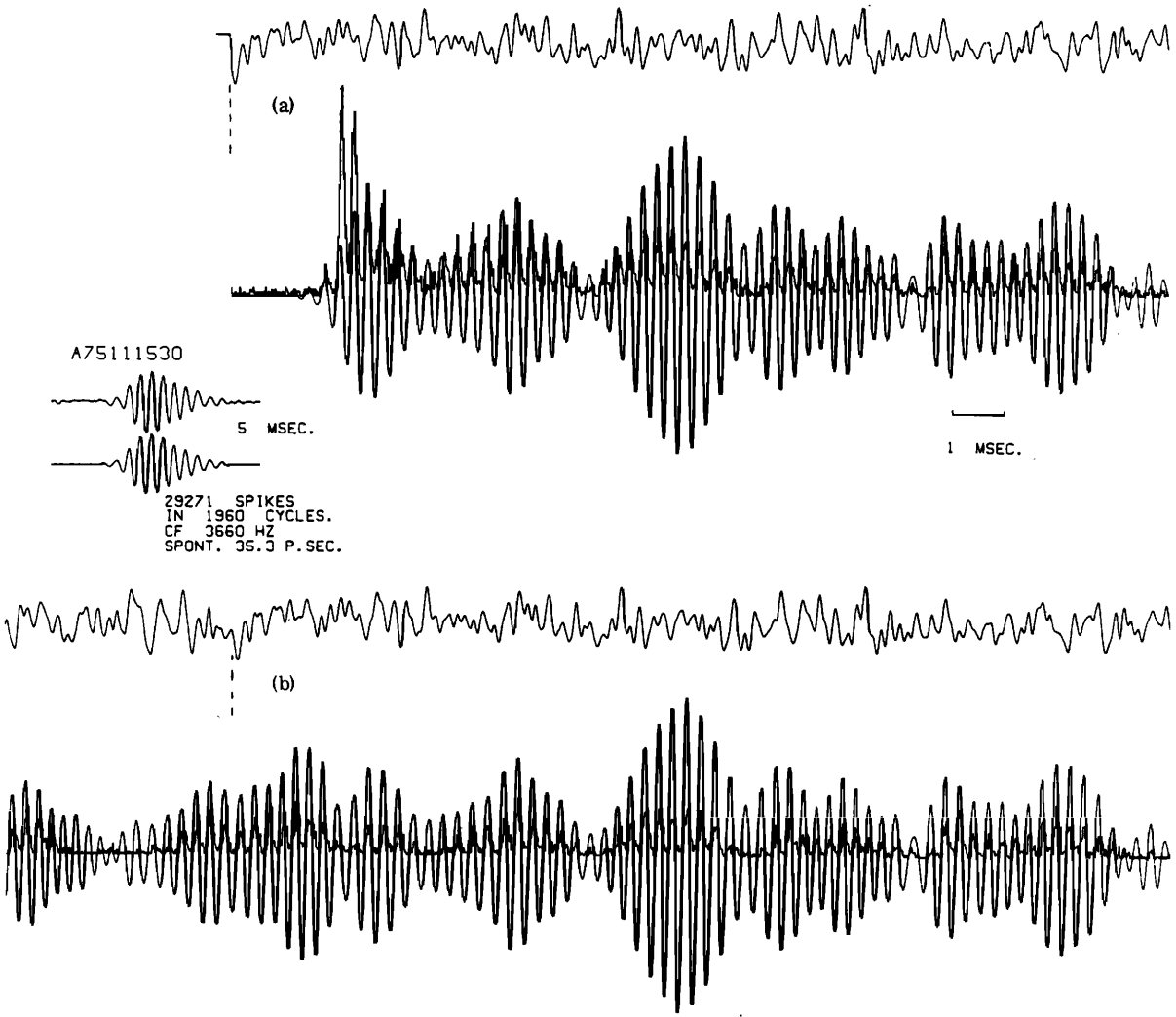

FIG. 14. Simulation result for a noise burst (a) shows the starting phase, and (b) shows a part of the recording where the waveform of the stimulus is exactly the same as in the starting phase. The dashed lines mark the beginnings of these sections. Unit nr.: 75-11-15, resonance frequency: 3.66 kHz, stimulus level: 30 dB (30 dB above threshold).

of average intensity we must take into account the dependence of the revcor function on intensity. For rapid variations we observe evidence of fast adaptation but only if the stimulus level changes rapidly over a large decibel range.

These two effects are the only manifestations of cochlear nonlinearity that are clearly present in our results. In view of known data on combination-tone generation and two-tone suppression we would have expected more evidence of nonlinearity, particularly of nonlinear filtering. Visual inspection of the simulation results in Sec. II does not yield clear manifestations of nonlinear filtering. The autocorrelation analysis of Sec. III reveals that the representation of the stimulus spectrum as it is processed by a primary auditory neuron is not noticeably different from a linear one. In the low-to-moderate intensity range, the nonlinearity that is responsible for the generation of combination tones and two-tone suppression seems to be of a type that does not affect frequency selectivity. At least, not for stimuli with a wide frequency spectrum. It seems safe to expect that this will hold true as long as the stimulus spectrum has slopes that are much lower than those of revcor amplitude spectra. (That is, it will hold for most, if not all, everyday sounds.) For these stimuli a linear transform of the stimulus is the principal controller of firing probability: the principle of specific coding (de Boer, 1973). Expressed in another way, this principle states that the components of a stimulus partake in the excitation of a neuron in relative proportions that are given by the neuron's revcor amplitude spectrum. This idea is consistent with findings on the near linearity of cochlear filtering obtained with quite different methods (Evans and Wilson, 1973).

It is most remarkable that the reverse correlation and the simulation method give so little evidence of nonlinear filtering. As far as the revcor function is concerned, this property can be understood. At present the model proposed by Pfeiffer (1970) comes nearest to the goal of describing all manifestations of cochlear nonlinearities. This model is composed of three independent elements in cascade: a first linear filter L_1, a no-memory nonlinear circuit NL, and a second linear filter L_2. This network should replace the linear network L in the mod-

el of Fig. 2. The filters L_1 and L_2 should be bandpass filters. A network of this type is known as a bandpass nonlinear (BPNL) network. A BPNL network has the curious property that for a Gaussian input the input–output cross-correlation function has a shape which is independent of the nature of the nonlinearity (de Boer, 1976a). This property can be considered as an extension of Price's theorem. It holds for any type of no-memory nonlinearity. A proof for the special case that the nonlinearity is an ideal rectifier, is implicit in the discussion of an extended primary neuron model by Johannesma *et al.* (1971). If the BPNL network really represents cochlear nonlinearity, the shape of the reverse-correlation function must be independent of stimulus intensity. This agrees with the general character of the experimental results for low-to-moderate intensities. However, the slight changes with intensity found in the revcor functions suggest that the model does not account completely for all manifestations of nonlinearity. That is, part of the nonlinearity is of a type that affects resonance directly, particularly at high stimulus intensities.

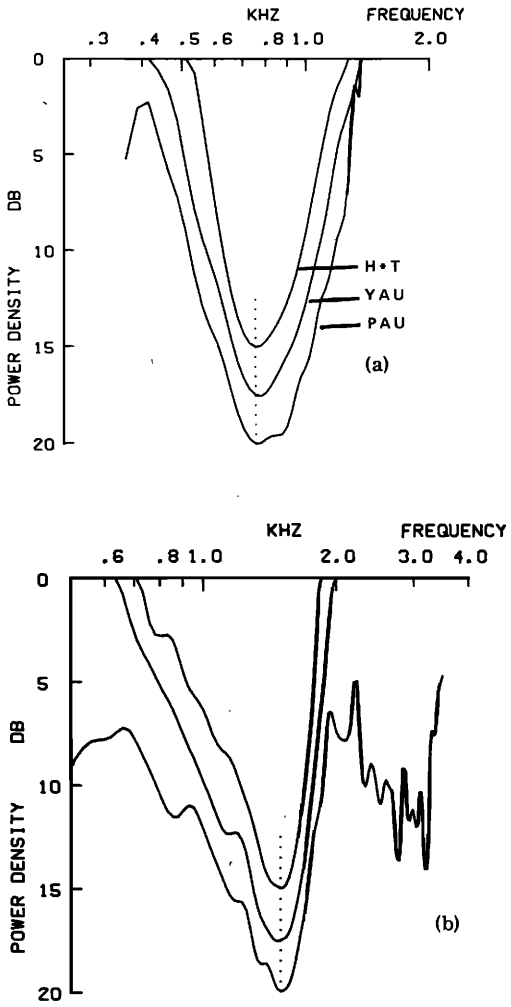

FIG. 15. Autocorrelation analysis applied to simulation result. Layout similar to the spectra of Figs. 5–8 but with a widened frequency scale, adapted to the resonance frequency and a different ordinate scale. See Appendix B. Symbols: PAU: acf of derectified $p(t)$ function (lowest curve), YAU: acf of $y^*(t)$ function (central curve), H^*T: power spectrum corresponding to $h^*(t)$-function (upper curve). (a) Unit nr.: 75-08-73, resonance frequency: 0.730 kHz, stimulation level: 35 dB/$\frac{1}{3}$ oct. See Fig. 10(a). (b) Unit nr.: 75-08-14, resonance frequency: 1.5 kHz, stimulation level: 50 dB/$\frac{1}{3}$ oct.

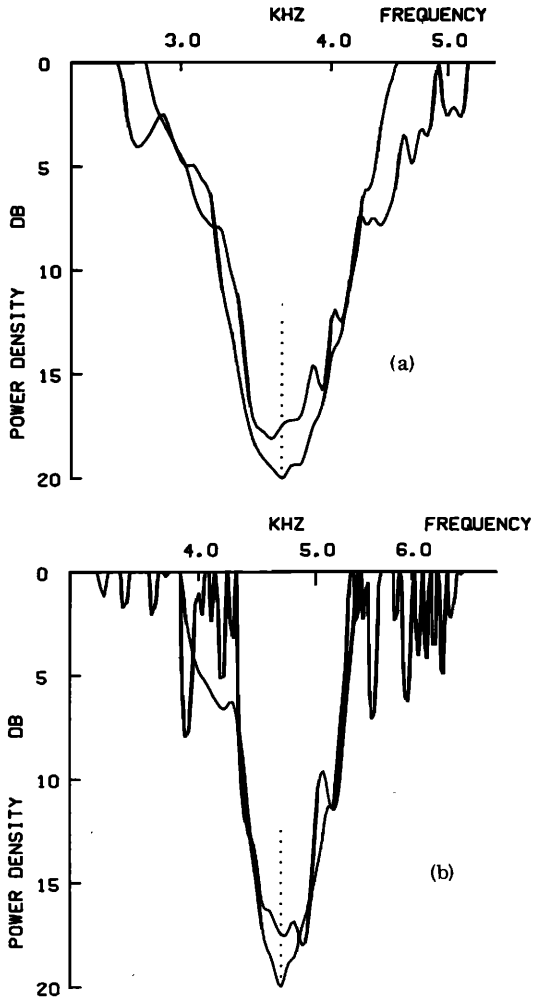

FIG. 16. As Fig. 15 but for two neurons with high resonance frequencies. Frequency scale still wider. (a) Unit nr.: 75-11-15, resonance frequency: 3.7 kHz, stimulation level: 30 dB/$\frac{1}{3}$ oct. See Fig. 14. (b) Unit nr.: 75-08-53 resonance frequency: 4.7 kHz, stimulation level: 30 dB/$\frac{1}{3}$ oct. See Fig. 12. Upper curve: PAU, lower curve: YAU, see legend to Fig. 15.

That the simulation results show so little influence of nonlinearity is more difficult to understand. A first indication is contained in the fact that the nonlinearity produces a compression which should be (almost) the same for all stimulus intensities. Then there is no reason why the timing of the output signal of the BPNL network would be different for identical stimulus signals differing only in intensity (cf. Davenport and Root, 1958). However, it is more difficult to understand why the waveform of the output signal of the nonlinear network would be so similar to that of the corresponding linear network. It can be ascertained that the BPNL network approximately has this property, provided narrow-band filtering occurs after the generation of distortion products and the stimulus is a signal with a larg-

er bandwidth. Furthermore, the output signal of a BPNL network has the same properties in its acf as are demonstrated for neural $p(t)$ functions in Sec. III, under the same conditions.

In any event, the observed scarcity of nonlinear effects is not due to the characteristic linearizing tendency of a correlation procedure. It seems to be more related to a fundamental property of wide-band noise signals processed by a nonlinear system like the cochlea. We remark that the analysis of Sec. III presents just one approach to the detection of nonlinearity effects. It is probable that a higher-order correlation analysis yields more evidence of nonlinear filtering although it is to be doubted whether the accuracy would be sufficient. In this connection we predict that much clearer manifestations of nonlinearity will show up if we stimulate with signals having spectra with steep slopes that are located asymmetrically with respect to the revcor spectrum. In particular, we recommend the use of single-sideband (SSB) signals with the carrier frequency at or near the resonance frequency (CF) of the neuron under study (cf. de Boer, 1976b). This is the reason we do not wish to pursue the analysis as presented in Sec. III to a greater depth or generality for wide-band stimuli. Nor do we deem it necessary to do this analysis for more neurons. Note, finally, that the signals commonly used to demonstrate generation of combination tones and two-tone suppression are really of the "SSB" variety: Their spectra are highly asymmetrical with respect to the resonance frequency.

We conclude with a few remarks on the *model* underlying the method of reverse correlation. The model of Fig. 2 is a stochastic one. It is remarkable that the simulation method reveals so little evidence of the threshold crossing that is inherent in a neural triggering process. Our earlier work on the reverse-correlation method was based on a model (Weiss, 1964, 1966) in which a threshold-crossing process was explicitly built in. From our results it appears that the mechanism of triggering of a primary auditory neuron is considerably more complicated than in the simple Weiss model, even in a modified form (de Jongh, 1973). In particular, the stochasticity of the mechanism is of a different kind.

Consider Figs. 11, 12, and 14 and observe the small but systematic differences between the shapes of the functions $y^*(t)$ and $p(t)$. The lobes of the firing probability function $p(t)$ are somewhat narrower than those of $y^*(t)$, and they appear as slightly, but significantly, skewed. These properties reveal that the model of Fig. 2 is not sufficiently detailed to describe nerve fiber timing patterns on a microtime scale. Johannesma *et al.* (1971) proposed and discussed a generalized model for a neuron that takes several physiological factors into account, such as: propagation of EPSP's along a primary dendrite and temporal integration at the site of initiation of nerve firings. A similar model can be used to represent a primary auditory neuron. Quite formally, the additional effects are represented by a linear transformation, namely, a low-pass filter, inserted between the rectifying nonlinearity NL and the pulse generator PG in Fig. 3. In a qualitative way, the observed discrepancies between $p(t)$ and $y^*(t)$ are consistent with such a model. Note that the theorem mentioned in connection with the BPNL network also applies to Johannesma's model, hence the cross-correlation function of the entire network relates directly to the response of the two linear systems in cascade. Since the secondary filter is a low-pass filter, it is readily understood that there is a high-frequency limit to the reverse-correlation method. More about the underlying model can be found in de Jongh's latest study (1977).

V. CONCLUSIONS

For the case of stimulation with wide-band signals the process of excitation of a primary auditory neuron can be split up into two parts (see Fig. 2), one involving linear filtering of the acoustical stimulus and the second one representing the generation of a stochastic series of pulses.

The impulse response of the linear filtering stage can be measured with the reverse-correlation method.

Revcor functions have very little phase modulation in their waveform and a gradual phase spectrum in the region of resonance (within 20 dB from the top).

The output signal of the linear filtering stage—the excitatory signal—is a good predictor of firing probability. Positive values give rise to increased firing probability, negative values produce suppression, even of spontaneous activity.

For wide-band stimuli, the spectral content—as measured from the autocorrelation function—of the firing probability is indistinguishable (within 1 dB) from that of the excitatory signal. That is, no trace of frequency-selective nonlinearity is observed. This holds for the range within 12–15 dB from the top of the power spectrum, and for the great majority of neurons tested. (More evidence of nonlinearity may be expected for single-sideband stimuli, etc.)

Neurons with resonance frequencies above 2.5 kHz show characteristic waveform differences between the firing probability and the—rectified—excitatory signal. Nevertheless, the conclusion above on the power spectrum remains valid.

When stimulus intensity varies rapidly over a large range, adaptation effects can be observed. These do not affect the timing pattern of the neuron's action potential but appear to control the (instantaneous) rate of firing in relation to the excitatory signal.

ACKNOWLEDGMENTS

The authors wish to acknowledge their gratitude to L. C. M. van Keulen, neurophysiologist. He did not only assist in neurophysiological matters concerning the experiments but was also a most valuable partner in numerous discussions, notably on details of modeling the processing that occur in primary auditory neurons. Since the latter topic is a subordinate one in the present paper, his influence on our thinking is not too obvious in this text but it will be in future papers (cf. de Jongh

1977). The electronic setup was supervised by C. Kruidenier on whom we could depend in all problems that arose in carrying out experiments.

APPENDIX A: DETAILS OF EXPERIMENTAL METHOD

The laboratory's PDP 9 computer is equipped with an ultrafast A/D conversion system and several especially designed types of interface to facilitate neurophysiological work. The A/D converter, Adage type VT 13 AB, has 14 bits of resolution and a conversion time of 5 μs. The 16-channel interface system (DEC AF 09) allows transfer rates of over 100 000 words/s controlled by an external clock. For the work reported in this paper the standard clock frequency was 50 kHz. A modification of the A/D system allows us to use one additional bit for labeling, in this way the instants at which nerve-fiber action potentials are detected are transferred to the computer's memory with a maximum error of one clock period. For less time-critical applications, "event detectors" are used that generate a program interrupt for each firing detected.

For the measurement of a revcor function the A/D system continually reads in the $x(t)$ signal. No sample is lost when the buffer is full and is starting to be refreshed from the bottom on. At each instant the immediate past of the signal is available and this can be used for the correlation computation according to Eq. (5). For this purpose the signal buffer is used as a circular buffer, i.e., the bottom is considered as the logical extension of the top. Several thousands of nerve firings are processed for each revcor function, using double-precision integer arithmetic.

The stimulus noise is generated with a Hewlett Packard noise generator type 3722 A operated with a bandwidth of 5 kHz. For the measurement of the revcor function the period of the noise is set to "infinite." To generate pseudorandom noise for studies with the simulation method the standard setting is "$N=13$." In that case the synchronization pulses are fed to the computer as well. The stimulus is fed to the ear via an earphone (Beyer DT 48) and a tube (91 mm long, 4.5-mm internal diameter). The earphone response is corrected with a filter so that it is flat within 5 dB when placed on a standard B & K artificial ear (type 4153) over the frequency range 300–8000 Hz. The tubing system introduces systematic variations of up to 7 dB and a typical resonance around 3 kHz. Until 1973 we measured the earphone response with the cat's ear *in situ* with help of a probe microphone. For the measurements reported in this paper we did not do this any more. As is stated in Sec. II, the electroacoustic transduction system is absorbed in the linear system L and for the comparison of the response to two different stimuli it is not necessary to correct for that. Such a correction would be necessary, of course, when we wish to relate properties of measured revcor functions to sound pressure at the eardrum. Still the variations in the shape of the revcor function or of its spectrum would be small, the main offender in this respect being the aforementioned resonance which can reach a peak of 10–15 dB (variable from animal to animal). The other wiggles in the frequency response are virtually without effect, compared to the other sources of measurement error.

The operation and preparation techniques are essentially those described by Kiang *et al.* (1965). We have left an alternative method (cf. de Boer, 1973) in favor of the "classical" method because of its greater yield. The microelectrode is directly driven by a remote-controlled stepping motor and reduction gear. Recorded signals are amplified by standard amplifiers. All signals—stimulus, response, and timing marks—are fed directly to the computer and are also stored on magnetic tape using an Ampex FR 1300 Instrumentation tape recorder. Tape speed was 30 or 60 in./s. In off-line processing of signals the tape speed was reduced by a factor of 4 or 8 to ensure that processing could keep up with the rate of input data.

Smoothing of revcor function was carried out in the time domain as well as in the frequency domain. Revcor functions were stored with a word count of 512 or 1024 and all truncation was carried out smoothly over a range of (at least) five successive points. Convolution, as is needed in the simulation procedure, was carried out via the fast Fourier transform routines developed for the PDP 9. When successive recordings are processed, as is needed in the simulation procedure, it is imperative that the read in of analog data occurs with exactly the same speed. For this reason we replaced the standard clock by a crystal-driven pulse generator operating at 50 kHz. A chain of dividers was used to accommodate processing with reduced tape speeds. A similar arrangement controls the tape speeds in the Ampex recorder.

In the presentation of the data we have continually used the convention that upward deflections in the revcor functions correspond to positive sound pressure. In the realm of polarity conventions, it is to be noted that using a nonlinear pulse generator PG in the model of Fig. 2 with a firing probability $p(t)$ that is a nondecreasing function of the excitatory signal $y^*(t)$, automatically results in the constant of proportionality C in Eq. (6) being a positive number.

APPENDIX B: DETAILS ON THE AUTOCORRELATION PROCEDURE

Consider two variables v_1 and v_2 with a joint Gaussian distribution having a correlation coefficient ρ_v (we leave out the dependence on τ here). Two other variables w_1 and w_2 are derived from v_1 and v_2 by ideal rectification: for positive v, w and v are equal, and for negative v, w is zero. The correlation coefficient ρ_w of w_1 and w_2 is

$$\rho_w = 2\int_0^\infty \int_0^\infty v_1 v_2\, p(v_1, v_2)\, dv_1\, dv_2 ,$$

where $p(v_1, v_2)$ is the probability density function of v_1 and v_2. The integrals can be evaluated analytically (Bussgang, 1952) and the result is

$$\rho_\omega = \pi^{-1}[(1-\rho_v)^{1/2} + \tfrac{1}{2}\rho_v \pi + \rho_v \tan^{-1}\rho_v/(1-\rho_v)^{1/2}] . \quad \text{(A1)}$$

Within an error of a few percent, this expression can be approximated by

$$\rho_w = (\rho_v + 1)^{1.62}/\pi \qquad \text{(A2)}$$

over the full range $-1 < \rho_v < +1$. Inversely, ρ_v can be expressed in terms of ρ_w:

$$\rho_v = (\pi\rho_w)^{0.617} - 1 \ . \qquad \text{(A3)}$$

This expression is used to convert the (normalized) autocorrelation function $\psi_p(\tau)$ of the firing probability $p(t)$ to the autocorrelation function $\psi_q(\tau)$ of a variable $q(t)$ that corresponds to v above. It is seen that this conversion—derectification—is very simple indeed.

If the signal $q(t)$ has the character of a narrow-band random signal, rectification has little effect on the spectrum in the main passband (cf. Davenport and Root, 1958), most of the distortion products arise elsewhere in the spectrum. Conversely, the derectification process has little effect in the main passband but it serves well—if not always satisfactorily in our recordings—to eliminate other distortion products due to rectification.

Records of the $y(t)$ and $p(t)$ signals are processed with a word count of 4000, the sampling period being 20 μs as usual. Autocorrelation functions are computed for 512 values of τ, starting at 0. A triangular window over the entire τ range is applied to achieve some smoothing in the frequency domain; next, the autocorrelation function is made symmetrical to a word count of 1024 and is Fourier transformed. The plotting program was similar to the one used for plotting revcor spectra; it had the option to widen the frequency scale and to adapt the center point to the resonance frequency. It should be noted that the vertical scale has acquired a different meaning: In the revcor spectrum plots the spectral amplitude is plotted on a decibel scale according to its power but in Figs. 15 and 16 the Fourier transform of the acf has the dimension of power (density) and can be plotted directly in decibels.

[1]We consider as a primary auditory neuron a functional unit that includes the external and the middle ear, the cochlea, the appropriate (inner) hair cell, and the process that leads to the production of an action potential in the associated nerve fiber. It transforms an analog signal—the acoustic waveform of the sound received—into a train of pulses ("events").

Allen, J. B. (1977). "Cochlear micromechanics-a mechanism for transforming mechanical to neural tuning within the cochlea," J. Acoust. Soc. Am. **62**, 930–939.

Anderson, D. J., Rose, J. E., Hind, J. E., and Brugge, J. F. (1971). "Temporal position of discharges in single auditory nerve fibers within the cycle of a sine-wave stimulus: frequency and intensity effects," J. Acoust. Soc. Am. **49**, 1131–1139.

Bussgang, J. J. (1952). "Crosscorrelation functions of amplitude-distorted Gaussian signals," MIT, RLE, Tech. Rep. No. 216.

Davenport, W. G., Jr., and Root, W. L. (1958). *An introduction to the theory of random signals and noise* (McGraw–Hill, New York), p. 295 ff.

de Boer, E. (1967). "Correlation studies applied to the frequency resolution of the cochlea," J. Aud. Res. **7**, 209–217.

de Boer, E. (1968). "Reverse correlation I," Proc. K. Ned. Akad. Wet. C **71**, 472–486.

de Boer, E. (1969a). "Encoding of frequency information in the discharge pattern of auditory nerve fibers," Int. Audiol. **8**, 547–556.

de Boer, E. (1969b). "Reverse correlation II," Proc. K. Ned. Akad. Wet. C **72**, 129–151.

de Boer, E. (1973). "On the principle of specific coding," J. Dyn. Syst. Meas. Control **95G**, 265–273.

de Boer, E. (1976a). "Cross-correlation function of a bandpass nonlinear network," Proc. IEEE **64**, 1443–1446.

de Boer, E. (1976b). "Spectral transformations by an infinite clipper," J. Acoust. Soc. Am. **60**, 960–963.

de Boer, E., and Jongkees, L. B. W. (1968). "On cochlear sharpening and cross-correlation methods," Acta Otolaryngol. **65**, 95–104.

de Boer, E., and de Jongh, H. R. (1971). "Computer simulation of cochlear filtering," in *Proceedings of the 7th International Congress on Acoustics* (Akademiai Kiado, Budapest), Vol. 3, 393–396.

de Boer, E., and Kuyper, P. (1968). "Triggered correlation," IEEE Trans. Biomed Eng. **BME-15**, 169–179.

de Jongh, H. R. (1972). "About coding in the VIIIth nerve," in *Proceedings of the IPO Symposium on Hearing Theory*, edited by B. L. Cardozo (Eindhoven, the Netherlands, pp. 70–77.

de Jongh, H. R. (1973). "Analysis of a spike generator," in *Proceedings of the 3d IFAC Symposium on Identification and System Parameter Estimation*, edited by P. Eyckhof (The Hague, the Netherlands), pp. 607–612.

de Jongh, H. R. (1977). "Models for the primary auditory neuron," (Doctoral dissertation (University of Amsterdam, the Netherlands) (to be published).

Duifhuis, H. (1972). *Perceptual analysis of Sound*, Doctoral dissertation (Eindhoven Technical University, the Netherlands).

Evans, E. F. (1972). "The frequency response and other properties of single fibers in the guinea-pig cochlear nerve," J. Physiol. London **226**, 263–287.

Evans, E. F. (1976). "Place coding of frequency and intensity in the peripheral auditory nervous system: pros and cons" (Invited paper XIII Int. Congr. of Audiology), Audiology (Basel) (to be published).

Evans, E. F. (1977). "Frequency selectivity at high signal levels of single units in cochlear nerve and nucleus," *Psychophysics and Physiology of Hearing*, edited by E. F. Evans and J. P. Wilson (Academic, London).

Evans, E. F., and Wilson, J. P. (1973). "Frequency selectivity of the cochlea," *Basic mechanisms in hearing*, edited by A. R. Møller (Academic, New York), pp. 519–551.

Goblick, T. J., and Pfeiffer, R. R. (1969). "Time-domain measurements of cochlear nonlinearities using combination click stimuli," J. Acoust. Soc. Am. **46**, 924–938.

Goldstein, J. L., and Kiang, N. Y.-S. (1968). "Neural correlates of the aural combination tone $2f_1 - f_2$," Proc. IEEE **56**, 981–992.

Grashuis, J. L. (1974). "The pre-event stimulus ensemble. An analysis of the stimulus-response relation for complex stimuli applied to auditory neurons" (Academic thesis, Nijmegen).

Gray, P. R. (1966). "A statistical analysis of electrophysiological data from auditory nerve fibers in cat," MIT, RLE, Tech. Rep. No. 451.

Hall, J. L. (1977). "Spatial differentiation as an auditory 'second filter.' Assessment on a nonlinear model of the basilar membrane," J. Acoust. Soc. Am. **61**, 520–524.

Hind, J. E., Anderson, D. J., Brugge, J. F., and Rose, J. E. (1967). "Coding of information pertaining to paired low-frequency tones in single auditory nerve fibers of the squirrel monkey," J. Neurophysiol. **30**, 794–816.

Johannesma, P. I. M., van Gisbergen, J. A. M., and Grashuis, J. L. (1971). "Forward and backward analysis of temporal relations between sensory stimulus and neural response," Internal Report (Lab. of Medical Physics, University of Nijmegen, the Netherlands).

Kiang, N. Y.-S., Watanabe, T., Thomas, E. C., and Clark, L. F. (1965). *Discharge patterns of single fibers in the cat's auditory nerve* (MIT, Cambridge, MA).

Kiang, N. Y.-S., and Moxon, E. C. (1974). "Tails of tuning curves of auditory nerve fibers," J. Acoust. Soc. Am. **55**, 620–630.

Pfeiffer, R. R. (1970). "A model for two-tone inhibition of single cochlear nerve fibers," J. Acoust. Soc. Am. **48**, 1373–1378.

Pfeiffer, R. R., and Kim, D. O. (1973). "Considerations of nonlinear response properties of single cochlear nerve fibers," *Basic mechanisms in hearing*, edited by A. R. Møller (Academic, New York, London), pp. 555–591.

Price, R. (1958). "A useful theorem for nonlinear devices having Gaussian inputs," IRE Trans. Inf. Theory **IT-4**, 69–72.

Rhode, W. S. (1971). "Observations of the vibration of the basilar membrane in squirrel monkeys using the Mössbauer technique," J. Acoust. Soc. Am. **49**, 1218–1231.

Rhode, W. S., and Robles, L. (1974). "Evidence from Mössbauer experiments for nonlinear vibration in the cochlea," J. Acoust. Soc. Am. **55**, 588–596.

Rose, J. E., Brugge, J. F., Anderson, D. J., and Hind, J. E. (1967). "Phase-locked response to low-frequency tones in single auditory nerve fibers of the squirrel monkey," J. Neurophysiol. **30**, 769–792.

Sachs, M. B. (1969). "Stimulus-response relation for auditory-nerve fibers: two-tone stimuli," J. Acoust. Soc. Am. **45**, 1025–1036.

Sachs, M. B., and Kiang, N. Y.-S. (1968). "Two-tone inhibition in auditory-nerve fibers," J. Acoust. Soc. Am. **43**, 1120–1128.

Siebert, W. M. (1968). "Stimulus transformations in the peripheral auditory system," in *Recognizing Patterns*, edited by P. A. Kolers and M. Eden (MIT, Cambridge, MA), pp. 104–133.

Smith, R. L. (1973). "Short-term adaptation and incremental responses of single auditory-nerve fibers," Special report LSC-S-11, Syracuse, NY.

Weiss, Th. F. (1964). "A model for firing patterns of auditory nerve fibers," MIT, RLE, Tech. Rep. No. 418.

Weiss, Th. F. (1966). "A model of the peripheral auditory system," Kybernetik **3**, 153–175.

Wilson, J. P., and Evans, E. F. (1971). "Grating acuity of the ear: Psychophysical and neurophysiological measures of frequency resolving power," in *Proceedings of the 7th International Congress on Acoustics* (Akademiai Kiado, Budapest), Vol. 3, pp. 397–400.

Wilson, J. P., and Johnstone, J. R. (1972). "Capacitive probe measures of basilar membrane vibration," in *Proceedings IPO Symposium on Hearing Theory*, edited by B. L. Cardozo (Eindhoven, the Netherlands), pp. 172–181.